

## Walks, Walls, Wetting, and Melting\*

Michael E. Fisher<sup>†</sup>

*Received October 6, 1983*

---

New results concerning the statistics of, in particular,  $p$  random walkers on a line whose paths do not cross are reported, extended, and interpreted. A general mechanism yielding phase transitions in one-dimensional or linear systems is recalled and applied to various wetting and melting phenomena in ( $d=2$ )-dimensional systems, including fluid films and  $p \times 1$  commensurate adsorbed phases, in which interfaces and domain walls can be modelled by noncrossing walks. The heuristic concept of an effective force between a walk and a rigid wall, and hence between interfaces and walls and between interfaces, is expounded and applied to wetting in an external field, to the behavior of the two-point correlations of a two-dimensional Ising model below  $T_c$  and in a field, and to the character of commensurate-incommensurate transitions for  $d=2$  (recapturing recent results by various workers). Applications of random walk ideas to three-dimensional problems are illustrated in connection with melting in a lipid membrane model.

---

**KEY WORDS:** Walks (random and vicious); walls (of domains and containers); wetting (transitions in two dimensions); melting (of adsorbed surface phases).

---

\* Based on the Boltzmann Medalist address presented at the 15th IUPAP International Conference on Thermodynamics and Statistical Mechanics, Edinburgh, July 1983.

<sup>†</sup> Baker Laboratory, Cornell University, Ithaca, New York 14853.

## CONTENTS

<b>1.</b>	<b>Introduction</b>	669
<b>2.</b>	<b>The Return of a Drunken Walker</b>	669
<b>3.</b>	<b>The Reunions of <math>p</math> Harmless Drunks</b>	672
<b>4.</b>	<b>Vicious Drunks and Their Reunions</b>	673
<b>5.</b>	<b>Absorbing Walls and the Death Factor</b>	678
	One walk and a wall: the method of images; two vicious walkers; many vicious walkers; two walkers and a wall; two dissimilar walkers; other aspects.	
<b>6.</b>	<b>Phase Transitions in Linear Systems</b>	684
<b>7.</b>	<b>Wetting of a Boundary Wall in Two Dimensions</b>	689
	Size and shape of a droplet on a wall; interface pinning in the bulk.	
<b>8.</b>	<b>Multiphase Systems: Interfacial Wetting</b>	694
	Two dimensional fluids; denaturation of a biopolymer; commensurate adsorbed phases; Chiral melting; Chiral clock models.	
<b>9.</b>	<b>The Forces between Walks and Walls</b>	703
<b>10.</b>	<b>Critical Prewetting</b>	708
<b>11.</b>	<b>Ising Model Correlations in Two Dimensions: Anomalous Decay Law</b>	712
<b>12.</b>	<b>Commensurate-Incommensurate Transitions</b>	716
<b>13.</b>	<b>Dislocations and Their Effects</b>	720
<b>14.</b>	<b>More than Two Dimensions? Lipid Membranes</b>	723
	<b>Acknowledgments</b>	727
	<b>References</b>	727

---

## 1. INTRODUCTION

The first lecture in a conference should stimulate rather than strain, should place a subject in perspective rather than delve into detail, should respect the history but survey recent happenings, and, ideally, should look on towards the future. In what follows I have endeavored to meet these specifications by revisiting the old but perennially alive topic of *random walks*. Some well known aspects will be recalled but fresh features will be exposed: in particular, the problem of  $p$  distinct walkers who interact will be discussed and some new asymptotic formulae, describing the “reunions of vicious walkers” and the effective forces between a walk and a wall and between walks themselves, will be presented. It transpires that these formulae can be applied to various problems on which recent researches in statistical physics and chemistry have focussed. Specifically, as I will demonstrate, one can give from a unified viewpoint, simple and easy derivations—admittedly mainly heuristic in character—for a range of exact theoretical results concerning wetting, melting, and other phenomena. The great wealth of results currently available is restricted to systems with only two infinite spatial dimensions: but such physical systems are increasingly open to penetrating experimental investigation. Nevertheless, one three-dimensional example is presented in the final section; however, the development of an analogous general approach for higher-dimensional systems remains a challenge for the future!

It should be mentioned that the primary purpose of this account of random walks and their applications is expository: however, one or two results not published (or in press elsewhere) do appear below.

## 2. THE RETURN OF A DRUNKEN WALKER

Consider a random walker in one dimension, say, a lone drunken Englishman who drops his house key on a long straight street and hunts for it. The displacement of the walker from the origin is measured by the coordinate  $x$ . For simplicity, we suppose that steps are taken at regular intervals,  $\Delta t = c$ , say, at each tick of a clock, so that the time for  $n$  steps is,

$$t = nc \tag{2.1}$$

For concreteness it is useful to suppose also that each step is of length  $a$  so that, equivalently, one may regard the walker as walking on a one-dimensional lattice of spacing  $a$ ; however, many results can be extended to a continuum in  $x$  and in  $t$ , and continuum language is the simplest to use, especially in discussing asymptotic behavior. It is also useful to regard “standing still” as a possible step and to associate *weights*,  $w_1$  for a positive

step,  $w_0$  for remaining still, and  $w_{-1} = w_1$  for a negative step. The total weight function, or generating function or partition function for a single step is then

$$e^{-\sigma} = w_1 + w_0 + w_{-1} \quad (w_{-1} = w_1) \quad (2.2)$$

Evidently the mean square step length is

$$b^2 = 2w_1e^{\sigma}a^2 \quad (2.3)$$

Of course, if  $w_0 = 0$ , as commonly considered, one has  $b = a$ . In order to simplify the appearance of expressions we will sometimes set  $b \equiv 1$  or, equivalently, suppose  $x$  is measured in units of  $b$ .

Now, as is well known, the total weight of all possible walks of  $n$  steps from the origin  $O$  ( $x = 0$ ), to the point  $x$  varies, asymptotically when  $n \rightarrow \infty$ , as<sup>(1)</sup>

$$Q_n^0(x) \approx e^{-\sigma n} e^{-x^2/2b^2n} / (2\pi b^2n)^{\frac{1}{2}} \quad (2.4)$$

If one takes  $w_1 = w_{-1} = 1$  and  $w_0 = 0$ , this corresponds simply to the number of distinct walks from  $O$  to  $x$ . We may regard  $Q_n^0(x)$  as a partition function or a partial partition function for an  $n$ -step walk. The total weight or total partition function is then just

$$Z_n^0 \equiv \int Q_n^0(x) dx = e^{-\sigma n} \quad (2.5)$$

Clearly, the scale of the distribution is set by

$$\tilde{x}_n = \sqrt{\langle x^2 \rangle_n} = bn^{\frac{1}{2}} \quad (2.6)$$

Now, by (2.4), the probability of return to the origin on the  $n$ th step (or, in a continuum description, to within a distance  $b$  of the origin) is

$$r_n = \frac{Q_n^0(0)}{Z_n^0} \approx \frac{1}{\sqrt{(2\pi)n^{\frac{1}{2}}}} \quad (2.7)$$

If our drunken Englishman dropped his key at the origin, traditionally located at the only lamp-post on the street, we would be interested in the probability of his eventual return to  $O$  after he continues walking indefinitely. This, and many similar questions, can be answered by employing a simple but basic probabilistic lemma<sup>(1)</sup> which we state as follows:

**Lemma.** Let  $p_n$ , with generating function

$$P(z) = \sum_{n=1}^{\infty} p_n z^n \quad (2.8)$$

be the probability that an event  $E$  occurs on the  $n$ th step (more generally, on the  $n$ th independent probabilistic trial). Then the probability,  $f_n$ , that  $E$  happens for the first time on step (or trial)  $n$  has the generating function

$$F(z) \equiv \sum_{n=1}^{\infty} f_n z^n = P(z)/[1 + P(z)] \tag{2.9}$$

The proof is simple and instructive: one merely notes that  $E$  either occurs for the first time on the last step,  $n$ , or happens sooner, say, for the first time on step  $l < n$ ; in that case  $E$  happens again on the  $n$ th step with probability  $p_{n-l}$ . Summing on the possible values of  $l$  thus yields the identity

$$p_n = f_n + f_{n-1}p_1 + f_{n-2}p_2 + \dots + f_1p_{n-1} \tag{2.10}$$

from which (2.9) follows directly. ■

Now the total probability that  $E$  eventually happens is given by

$$\begin{aligned} F_{\infty} &\equiv f_1 + f_2 + \dots \equiv \sum_{n=1}^{\infty} f_n \\ &= F(1) = P(1-)/[1 + P(1-)] \end{aligned} \tag{2.11}$$

where the notation  $z = 1 -$  implies the limit  $z \nearrow 1$ . Let us, for concreteness, suppose, as will often be true, that  $p_n$  obeys an asymptotic power law, say,

$$p_n \approx p_0/n^{\psi} \quad (\psi > 0) \tag{2.12}$$

Then  $P(1 -) = \infty$  if and only if  $\psi \leq 1$ . Consequently, the lemma yields the following.

**Corollary.** Let (2.12) describe the probability of event  $E$  occurring on the  $n$ th trial. Then, when  $n \rightarrow \infty$ ,

(a) if  $\psi \leq 1$ , the event  $E$  occurs with probability one, i.e., is “certain” to occur (and, in fact, occurs infinitely often<sup>(1)</sup>); but

(b) if  $\psi > 1$  the event  $E$  is *not certain*, failing to occur with a probability  $1/[1 + P(1 -)] > 0$ .

It is not hard to see that in case (a) one has  $f_n \sim 1/n^{2-\psi}$ ; conversely,  $\psi > 1$  yields  $f_n \sim 1/n^{\psi}$  (where, as sometimes below, we neglect the possibility of extra logarithmic factors in asymptotic behavior on borderlines).

Finally, returning to our lone drunken Englishman, we see from (2.7) that  $\psi = \frac{1}{2}$  describes his probability of return: thus he is *certain* to return eventually and the probability that he returns for the first time on the  $n$ th step decays as  $f_n \sim 1/n^{3/2}$ .

### 3. THE REUNIONS OF $p$ HARMLESS DRUNKS

Let us now give our drunken Englishman two more drunk but otherwise harmless companions, say an Indian and a Japanese. Suppose they start at, or near, the lamp-post at  $O$  and exchange keys cyclically (say,  $E \Rightarrow I \Rightarrow J \Rightarrow E$ ) before wandering off in random fashion. In order that each one can recover his own key in a "fair exchange," i.e., such that all parties in an exchange are left equally happy, all three must meet together again somewhere at the same time, enjoy their *reunion*, and recycle the keys! What is the probability that such a reunion occurs on the  $n$ th step? Is an eventual reunion certain? More generally, what happens if  $p$  drunks, with coordinates  $x_1, x_2, \dots, x_p$ , exchange their keys cyclically and walk off in the hopes of eventual reunion?

In formulating this question "harmless" has been used in a technical sense, specifically, to mean that our walkers may pass each other or occupy the same lattice site freely without harm, or, more explicitly, without change in the overall statistical weight. Since each walker is, thus, independent of the others the total weight of walks of  $n$  steps (by *each* walker) all starting at  $O$  and, collectively, proceeding to  $\vec{x} = (x_1, x_2, \dots, x_p)$  is simply

$$Q_n^p(\vec{x}) = \prod_{j=1}^p Q_n^0(x_j) \approx \frac{e^{-p\pi n} e^{-|\vec{x}|^2/2n}}{(2\pi n)^{\frac{1}{2}p}} \quad (3.1)$$

where, now, we have taken  $b = 1$  for brevity. The significant feature of this formula for us resides mainly the exponent,  $\frac{1}{2}p$ , in the denominator.

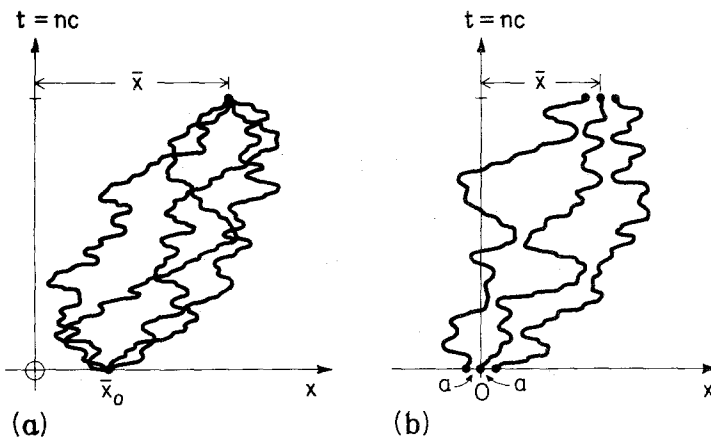


Fig. 1. Illustrations of (a) a reunion of  $p = 4$  harmless, or noninteracting, walkers whose paths may cross; (b) a reunion of  $p = 3$  interacting walkers whose paths may *not* cross.

From the basic distribution (3.1) we see directly that the probability of a reunion at  $x_1 = x_2 = \dots = x_p = \bar{x}$  on the  $n$ th step if all walkers started at  $\bar{x}_0$  (see Fig. 1a) is

$$r_n(\bar{x}) \sim e^{-p(\bar{x} - \bar{x}_0)^2/2n} / n^{\frac{1}{2}p} \quad (3.2)$$

The Corollary of the previous section thus tells us that a reunion at any fixed position,  $\bar{x}$ , is *certain* if  $p = 2$  but is *uncertain* for  $p \geq 3$ .

If our drunks do not care *where* they meet again we need the *probability of a reunion anywhere*. To this end, we should integrate as follows:

$$R_n^p = \int d\bar{x} r_n(\bar{x}) = n^{\frac{1}{2}} \int d\bar{X} r_n(n^{\frac{1}{2}}\bar{X}) \quad \text{with } \bar{X} = \bar{x}/n^{\frac{1}{2}} \quad (3.3)$$

where  $X \equiv x/n^{\frac{1}{2}}$  is the appropriately scaled distance coordinate for  $n$ -step walks: integration thus cancels a factor  $n^{\frac{1}{2}}$  in the denominator of (3.2) and yields

$$R_n^p \sim 1/n^{\frac{1}{2}(p-1)} \quad (3.4)$$

Hence the eventual reunion anywhere of  $p$  harmless drunks is *certain* if  $p = 2$  or 3 but *uncertain* for  $p \geq 4$ .

Evidently, it is easy to deal with harmless drunks: in statistical mechanical terms they correspond simply to *noninteracting* walkers. As such they are hardly more interesting than an ideal gas. Thus we turn to *interacting walkers*.

#### 4. VICIOUS DRUNKS AND THEIR REUNIONS

The most natural interactions to consider between different walkers are short-range or contact interactions which, in particular, do not allow one walker to pass another. Then, if the  $p$  walkers are labelled in linear sequence so that one has

$$x_1 < x_2 < \dots < x_p \quad (4.1)$$

at time  $t = 0$ , these same inequalities hold for all subsequent times. This restriction, which we henceforth adopt, is not, however, sufficient to specify the nature of the interactions in full: one must, in addition, say what weights are to be attached to the paths of two colliding walkers after a collision.

One straightforward possibility is to *replace* any forbidden steps, resulting, for example, in two adjacent walkers landing on the same site, by *alternative allowed steps*. The total weight of all walks would then be preserved, the weight of the forbidden collision steps being transferred to the associated allowed steps. Such walkers might be termed *bouncy walk-*

ers: they will bounce off one another, and hence satisfy (4.1), but, statistically, they will tend to remain close to one another because of the increased weight of sequences with many near-collisions. Such bouncing walks can be discussed by the techniques explained below; however, for statistical mechanical applications they seem of less value than the complementary assignment of post-collision weights by which we characterize vicious drunken walkers.

*Vicious drunks* shoot on sight—we refrain from speculating as to their national origins—but they are short-sighted: thus on arriving at the same site they shoot each other dead: otherwise, they do not interact. In formal terms, the allowed steps carry the same weights,  $w_1$ ,  $w_0$ , or  $w_{-1}$ , as before but any forbidden walks with multiple site-occupancy are assigned weight zero. Clearly, the paths of vicious walkers do not cross so that (4.1) is certainly maintained. Three specific models can be handled explicitly in closed form:

(A) *Lock step*. The walkers start either on the even- or the odd-numbered sites of the lattice: at each tick of the clock *each walker moves* either to the right or to the left with weight  $w_1 = w_{-1}$  (and  $w_0 = 0$ ) subject to no two walkers occupying the same site at the same time. (See Fig. 2a.)

(B) *Random turns*. The walkers start at distinct but otherwise arbitrary lattice sites: at each tick of the clock a *randomly chosen* walker takes a

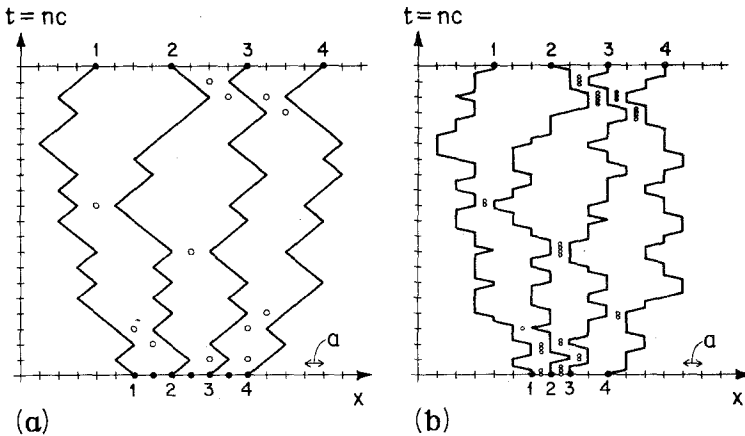


Fig. 2. Sample paths for lattice models of vicious walkers for: (a) the lock step model, (A), in which all  $p = 4$  walkers start on even-numbered sites and all move at the same moments; and (b) the random model, (B), where walkers can start on any site but only one moves at a time. In this illustration, the *average rate* at which a single walker steps has been chosen to be the same in both models. The open circles mark situations (“close calls”) in which, owing to the proximity of another walker, the allowed steps are limited.

random step (with weights  $w_0, w_1 = w_{-1}$ ) subject to no two walkers occupying the same site at the same time. (See Fig. 2b.)

(C) *Brownian motion.* The continuum limit in  $x$  and  $t$  may be taken formally in model (A) or (B).

The reason why these particular models are tractable will become clear below.

Now we may ask: “What is the probability that all walkers survive for  $n$  steps?” “What is the spatial distribution of the survivors?” “What is the probability of a *reunion* in which all walkers start close to (but not *at*) the origin, say, at spacing  $a$ , as illustrated in Fig. 1b and, after  $n$  steps, *all* meet again, not *on the same* site but, say, at spacing  $a$  at mean position  $\bar{x}$ ?” The basic message is that all these questions can be answered exactly in closed form! To preview some of the principal results, the probability that  $p$  walkers survive for  $n$  steps decays asymptotically as

$$P_n^{(p)} \sim 1/n^{\frac{1}{4}p(p-1)} \tag{4.2}$$

The probability of a reunion anywhere on the  $n$ th step varies as

$$R_n^{(p)} \sim 1/n^{\frac{1}{2}(p^2-1)} \quad \text{as} \quad n \rightarrow \infty \tag{4.3}$$

The exponent in this expression,

$$\begin{aligned} \psi_p = \frac{1}{2}(p^2 - 1) = 0, \quad \frac{3}{2}, \quad 4, \quad 7\frac{1}{2}, \quad \dots & \quad \text{for} \\ p = 1, \quad 2, \quad 3, \quad 4, \quad \dots & \end{aligned} \tag{4.4}$$

turns out to be the principal fact needed in most of the applications.

It follows from (4.2) and (4.3) that the (conditional) probability that the survivors enjoy a reunion on the  $n$ th step behaves as

$$S_n^{(p)} = R_n^{(p)} / P_n^{(p)} \sim 1/n^{\frac{1}{4}(p-1)(p+2)} \tag{4.5}$$

as  $n \rightarrow \infty$ . A reunion is thus certain for  $p = 2$ , which is not so surprising in view of the result for two harmless walkers; however, a reunion of vicious walkers is *not* certain for  $p \geq 3$ , a fact which seems less than obvious. (Recall that three harmless walkers are certain to have a reunion.)

These results follow by asymptotic analysis of an exact general expression<sup>1</sup> for the distribution of  $p$  vicious walkers which is explained in the next section; however, this is a convenient point at which to present some of the more useful exact results.<sup>2</sup> Consider, for simplicity, the situation in which

<sup>1</sup> The basic mathematical result was derived and analyzed in connection with a study by Huse and Fisher<sup>(2)</sup> of fluctuations near a commensurate-incommensurate transition in two-dimensional systems (see also below); although only fairly standard methods of analysis are entailed, the general problem seems not to have been considered previously in the literature.

<sup>2</sup> A reader unconcerned with the details may skim the rest of this section and refer back to particular results only as needed.

the  $p$  walkers are, initially, *equispaced*: with no loss of generality for the asymptotic behavior we may suppose the spacing is  $a$  and take the initial coordinates as

$$\vec{x}_0 = (x_{j,0}) \quad \text{with} \quad x_{j,0} = (j - 1)a, \quad j = 1, 2, \dots, p \quad (4.6)$$

Then, as  $n \rightarrow \infty$ , the *asymptotic distribution* for the lattice models is found to be

$$Q_n^{(p)}(\vec{x}) \approx \frac{e^{-pon} e^{-|\vec{x}|^2/2n}}{(2\pi n)^{\frac{1}{2}p}} e^{-a^2 s_p/n} \prod_{j>k \ge 1}^p (e^{ax_j/n} - e^{ax_k/n}) \quad (4.7)$$

where  $s_p = \frac{1}{12}p(p - 1)(2p - 1)$  and again, we take  $b \equiv 1$ : the inequalities (4.1) are understood. The leading factor here is identical with the expression for harmless walkers: see (3.1). The second factor yields a negligible correction when  $n \rightarrow \infty$ . The crucial feature is thus the final “death factor” which, itself, is a product of  $\frac{1}{2}p(p - 1)$  factors, one factor,  $D_{jk}$ , for each pair of walkers,  $(j, k)$ . Note also that (4.7) is exact for the continuum model (C).

Suppose now we are interested in the probability that all  $p$  walkers survive to the  $n$ th step. This can be obtained from (4.7) by integrating on each of the  $p$  final coordinates,  $x_j$ , subject, as always, to (4.1). Rescaling with  $X_j = x_j/n^{\frac{1}{2}}$ , as in (3.3), cancels the factor  $n^{-\frac{1}{2}p}$ ; as  $n \rightarrow \infty$ , the individual death factors then yield

$$D_{jk} = e^{ax_j/\sqrt{n}} - e^{ax_k/\sqrt{n}} \approx a(X_j - X_k)/n^{\frac{1}{2}} \quad (4.8)$$

The overall death factor thus generates a factor  $n^{-\frac{1}{4}p(p-1)}$  just as quoted in (4.2). More explicitly, the *probability of survival* may be written

$$P_n^{(p)} = A_p n^{-\frac{1}{4}p(p-1)} [1 + O(p^3 a^2/b^2 n)] \quad (4.9)$$

as  $n \rightarrow \infty$ , with amplitude

$$A_p = \left(\frac{a}{b}\right)^{\frac{1}{2}p(p-1)} \int \frac{d\vec{X}}{p!} \frac{e^{-\frac{1}{2}|\vec{X}|^2}}{(2\pi)^{\frac{1}{2}p}} \prod_{(j,k)} |X_j - X_k| \quad (4.10)$$

For dimensional consistency the length  $b$  has now been exhibited. The integral on  $\vec{X}$ , which is a pure number, runs over *all* real values of the  $X_j$  while the product runs over all  $\frac{1}{2}p(p - 1)$  distinct pairs  $(j, k)$ : for fixed values of  $p$  is not hard to evaluate the integral more explicitly.

The *probability of a reunion* at  $\vec{x}$  also follows directly from (4.7): thus for the *equispaced* final positions

$$x_j - x_k = (j - k)a' \quad \text{with} \quad \bar{x} = \sum_{j=1}^p x_j/p \quad (4.11)$$

each death factor varies, for large  $n$ , as  $aa'/n$  [see (4.8)] and so one finds

$$r_n^{(p)}(\bar{x}) \approx B_p e^{-p(\bar{x}-\bar{x}_0)^2/2n} / n^{\frac{1}{2}p^2} \tag{4.12}$$

where  $\bar{x}_0$  is defined in analogy with  $\bar{x}$ . If one starts from (4.7) [rather than directly invoking (4.8)] one finds

$$B_p \approx \frac{e^{-(a-a')^2 s'_p/n}}{(2\pi)^{\frac{1}{2}p}} \prod_{k=1}^p (1 - e^{-aa'k/n})^{p-k} \tag{4.13}$$

where  $s'_p = \frac{1}{24}p(p^2 - 1)$ . For large  $n$  this simplifies to

$$B_p = (2\pi)^{-\frac{1}{2}p} \left( \frac{aa'}{b^2} \right)^{\frac{1}{2}p(p-1)} \left( \prod_{q=1}^{p-1} q! \right) \left[ 1 + O\left( \frac{p^3 aa'}{b^2 n} \right) \right] \tag{4.14}$$

The expression (4.12) holds more generally for the probability of a reunion for *arbitrary* fixed initial positions,  $x_{j,0}$ , and final positions,  $x_j$ , if the amplitude is replaced by<sup>3</sup>

$$B_p(\vec{x}, \vec{x}_0) = \frac{\prod_{j>k \geq 1}^p (x_j - x_k)(x_{j,0} - x_{k,0})}{(2\pi)^{\frac{1}{2}p} b^{p(p-1)} 1! 2! \cdots (p-1)!} \left[ 1 + O\left( \frac{p^3 a^2}{b^2 n} \right) \right] \tag{4.15}$$

To find the probability of a reunion *anywhere* we merely need to integrate (4.12) on  $\bar{x}$ . As in (3.3), this generates a factor  $n^{-1/2}$  and so confirms the important conclusion (4.3); more explicitly, one obtains

$$R_n^{(p)} = C_p / n^{\frac{1}{2}(p^2-1)} \left[ 1 + O\left( \frac{p^3 a^2}{b^2 n} \right) \right] \tag{4.16}$$

with amplitude

$$C_p = \frac{(a/b)^{p(p-1)} \prod_{q=1}^{p-1} q!}{(2\pi)^{\frac{1}{2}p(p-1)} \sqrt{p}} \tag{4.17}$$

It is natural, finally, to enquire if these exact results might not be extended, say, in models (B) and (C), to *dissimilar walkers*, with, in particular, *distinct diffusivities* as measured by their mean square single step lengths,  $b_i^2$ . In general it seems difficult to obtain comparable explicit formulae. However, for the simplest nontrivial case of two walkers progress can be made by the methods to be explained. For the continuum model, (C), the exact result can be expressed conveniently as

$$Q_n^{(2)}(\vec{x}) = e^{-(\sigma_1 + \sigma_2)n} \frac{e^{-(\bar{x}-\bar{x}_0)^2/\bar{b}^2 n}}{2\pi \bar{b}^2 n} (1 - e^{-aa'/\bar{b}^2 n}) e^{-(a-a')^2/4\bar{b}^2 n} \tag{4.18}$$

<sup>3</sup> This result follows by analyzing the general result presented in the next section.

where the mean position and diffusivity are defined by

$$\bar{x} = \frac{1}{2} \left( \frac{b_2}{b_1} x_1 + \frac{b_1}{b_2} x_2 \right) \quad \text{and} \quad \bar{b}^2 = \frac{1}{2} (b_1^2 + b_2^2) \quad (4.19)$$

while, with no loss of generality, we have, as before

$$x_2 = x_1 + a' \quad \text{and} \quad x_{2,0} = x_{1,0} + a \quad (4.20)$$

When  $b_1 = b_2$  all the previous results for  $p = 2$  are easily recaptured.

## 5. ABSORBING WALLS AND THE DEATH FACTOR

### 5.1. One Walk and a Wall: The Method of Images

In order to understand the origin and form of the death factor in the interactions of vicious walkers and, thereby, derive the results of the previous section, consider a single random walker who walks near a wall located at the origin. We take the wall to be an *absorbing wall* in the sense that no walk may penetrate the wall and any walk attempting to do so is eliminated. In our anthropomorphic picture, we may visualize an absorbing wall as a *cliff* over which a drunken walker may fall to his death! The interactions between wall and walker are, thus, completely analogous to those between vicious walkers. (We could, equally, discuss a *reflecting wall* which would correspond to *bouncy* walkers.)

To be concrete, suppose the wall is located at the origin,  $x = 0$ , and a walker starts from  $x_0 = a$ . We ask for the weight of all  $n$ -step walks to  $x$  ( $> 0$ ) which have never visited the region  $x \leq 0$ . This is a standard random walk problem<sup>(1)</sup> which is readily solved by the method of images. To review this technique consider Fig. 3, which shows two possible  $n$ -step walks from  $x_0 = a$  to  $x$ . The walk labelled (i) is allowed since it does not touch or cross the wall; by contrast walk (ii) crosses the wall and should be eliminated. To this end suppose walk (ii) *meets* or *hits* the wall for the first time on step  $n_1$  and consider the modified walk, (iii), formed by reflecting in the origin,  $O$ , i.e., in the wall, all steps from 0 to  $n_1$ . As illustrated in Fig. 3 this yields an *image walk* which starts at  $x_0 = -a$ , the image of the original starting point, meets the wall on step  $n_1$ , and reaches  $x$ , the original endpoint, on step  $n$ . It is evident that each such walk from  $x_0 = -a$  to  $x > 0$  matches a unique forbidden walk from  $x_0 = a$  to  $x > 0$ . Consequently, if  $Q_n^0(x, x_0)$  is the weighted number or partition function for free  $n$ -step walks, the corresponding number/partition function for walks in the presence of the absorbing wall is exactly

$$Q_n^W(x, a) = Q_n^0(x, a) - Q_n^0(x, -a) \quad (5.1)$$

where the second term represents the "negative" image walks.

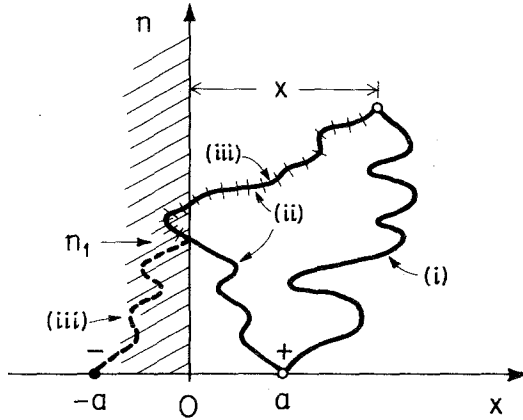


Fig. 3. Walks starting from  $x_0 = a$  in the presence of an absorbing wall at  $x = 0$ . Walk (i) is allowed. Walk (ii) is forbidden, since it meets the wall on step  $n_1$ , but may be cancelled by the partially reflected, negative wall (iii) which starts at  $x_0 = -a$ .

Now, quite generally, if

$$\Phi(\theta) = \sum_l w_l e^{i l \theta} \tag{5.2}$$

is the single-step partition function or generating function for a free walk on a lattice, one has, in the standard way,<sup>(1)</sup>

$$Q_n^0(l_a, l_0 a) = \int_{-\pi}^{\pi} \frac{d\theta}{2\pi} e^{-i(l-l_0)\theta} [\Phi(\theta)]^n \tag{5.3}$$

from which, for example, one easily derives the usual explicit binomial expressions for walks with only nearest-neighbor jumps. Likewise, when  $b^2 < \infty$ , a steepest descent argument yields the basic continuum result, (2.4), as  $n \rightarrow \infty$ . Notice, however, that the argument leading to (5.1) presupposes that any walk reaching  $x < 0$  must intersect the wall at  $x = 0$ . This tacit hypothesis is valid for Brownian motion, i.e., for a continuum walk, but fails for a lattice walk if, in a single step, the walker can jump more than one lattice spacing. This fact underlies the restrictions to models (A) and (B) in the previous section; but see also below.

Since our primary interest is in asymptotic behavior let us utilize (2.4) or, in order to write equalities adopt the continuum model, (C). Then (5.1), with  $b = 1$ , yields

$$\begin{aligned} Q_n^W(x, a) &= \frac{e^{-an}}{(2\pi n)^{\frac{1}{2}}} \left[ e^{-(x-a)^2/2n} - e^{-(x+a)^2/2n} \right] \\ &= \frac{e^{-an} e^{-x^2/2n}}{(2\pi n)^{\frac{1}{2}}} e^{-a^2/n} (e^{ax/n} - e^{-ax/n}) \end{aligned} \tag{5.4}$$

The last expression here has a close resemblance to (4.7), the basic result for  $p$  initially equispaced vicious walkers: evidently the death factor describes simply the interference between the free walk and the negative image walk required to eliminate the forbidden walks which would cross the wall. As we will show, the same mechanism accounts for the death factor in all the other cases.<sup>4</sup>

When  $a$  is fixed and  $n \rightarrow \infty$  the exact (continuum) result simplifies to

$$Q_n^W(x) \approx \frac{e^{-an}}{\sqrt{(\pi/2)}} \frac{axe^{-x^2/2n}}{n^{3/2}} \quad (5.5)$$

which reveals the distribution of a walk near a wall. Setting  $x = a$  then shows that the number of returns of a walk to the wall varies as

$$R_n^W \approx C^W / n^{3/2} \quad (5.6)$$

If one appends a zeroth step from  $O$  to  $x_0 = a$  and adds an  $(n + 1)$ th step from  $x = a$  to  $O$  this result equally describes walks which leave the origin on step zero and return *for the first time* on step  $n + 1$ : it is thus reassuring to confirm that the exponent  $3/2$  in (5.6) is precisely what follows from the Lemma and Corollary in Section 1! One also notices that this exponent characterizes the reunions of  $p = 2$  vicious walkers [see (4.3)]. This is no accident since one may regard a rigid absorbing wall as the limiting case of a vicious walker whose diffusivity vanishes, i.e.,  $b_1^2 \rightarrow 0$ , so that he does not move. Indeed, if one calculates the reunions of two dissimilar walkers from (4.18) by integrating (4.18) with respect to  $\bar{x}$  and then sets  $b_1 = 0$ ,  $b_2 = b = 1$ ,  $\sigma_1 = 0$ ,  $\sigma_2 = \sigma$  and  $a' = x$  one reproduces (5.5) precisely for  $n \rightarrow \infty$ .

## 5.2. Two Vicious Walkers

Consider now, on its own merits, the case of  $p = 2$  identical vicious walkers on the line (and in the absence of a wall).<sup>5</sup> Two coordinates,  $x_1$  and  $x_2$ , are needed and they are subject to the restriction  $x_1 < x_2$ . We may, however, regard  $x_1$  and  $x_2$  alternatively as the coordinates of a *single*, new *compound walker* who walks in a *plane*. Furthermore, the restriction  $x_1 < x_2$  then translates into an *exclusion* of our two-dimensional walker from the line  $x_1 = x_2$  and from the half-plane lying below the line, as illustrated in Fig. 4. In other words, we again have a single walker and an absorbing wall

<sup>4</sup> A reader accepting this but more interested in the applications will lose little by perusing the next two paragraphs and then skipping to Section 6.

<sup>5</sup> For further details, especially for lattice models, see Huse, Szpilka, and Fisher<sup>(3)</sup>; Huse and Fisher.<sup>(2)</sup>

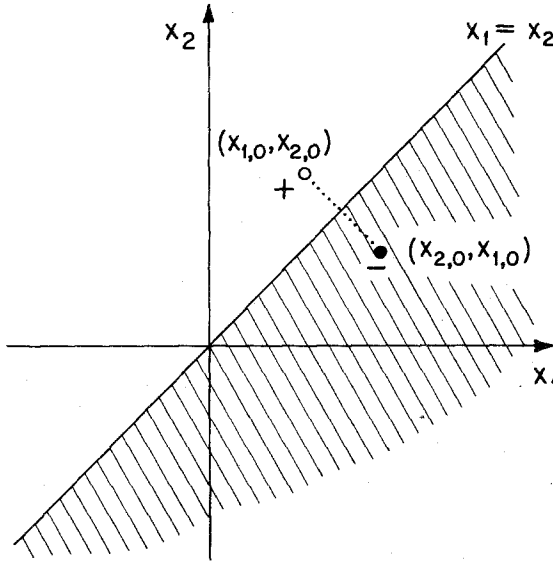


Fig. 4. The plane  $(x_1, x_2)$  of the compound walker for  $p = 2$  vicious walkers showing the starting point  $(x_{1,0}, x_{2,0})$ , the wall/mirror plane,  $x_1 = x_2$ , and the corresponding image-walker starting point. The combination of original and image walks satisfies the constraint  $x_1 < x_2$ .

but, now, in two dimensions. This may be solved just as before. If the compound walker starts at  $\vec{x}_0 \equiv (x_{1,0}, x_{2,0})$  the negative, image walker must start at  $\vec{x}'_0 = (x_{2,0}, x_{1,0})$ : see Fig. 4; the analog of (5.1) then holds precisely. However, the behavior of the free lattice walks is now given by the generalization of (5.3) to two dimensions. For models (A) and (B) the corresponding single-step generating functions are easily seen to be

$$\Phi_A(\theta_1, \theta_2) = w_1^2 (e^{i\theta_1} + e^{-i\theta_1})(e^{i\theta_2} + e^{-i\theta_2}) \tag{5.7}$$

$$\Phi_B(\theta_1, \theta_2) = w_0^2 + w_0 w_1 (e^{i\theta_1} + e^{-i\theta_1} + e^{i\theta_2} + e^{-i\theta_2}) \tag{5.8}$$

respectively, and one may check<sup>(3)</sup> that a compound walker starting with  $x_{1,0} < x_{2,0}$  cannot reach the half-plane  $x_1 > x_2$  without passing through a site on the diagonal  $x_1 = x_2$ , i.e., without intersecting the wall, as required for the validity of the method.<sup>6</sup> Asymptotically, the distribution for a compound walker in  $d$  dimensions is simply the product of the distributions

<sup>6</sup> Notice that in model A the generating function factorizes, which means that walkers far apart move independently, as desirable for physical applications. This is not the case in model B, other than in a statistical sense, since the second walker may not move on the same tick of the clock as the first walker.

for  $d$  one-dimensional walkers [and so is given by (3.1) with  $p = d$ ]. On putting everything together we achieve a derivation of (4.7) for the case  $p = 2$  (the equispaced condition then being no restriction).

### 5.3. Many Vicious Walkers

The problem of  $p > 2$  vicious walkers can, with a little more care, be handled similarly.<sup>(2)</sup> One considers a single compound walker in  $p$  dimensions moving subject to the coordinate constraints  $x_j < x_k$  for  $j < k$ , all  $(j, k)$ . This translates into  $\frac{1}{2}p(p-1)$  walls,  $x_j = x_k$ , in  $p$ -space which is thereby divided into  $p!$  disjoint segments corresponding to the permutations,  $\hat{\pi}$ , of labels in the inequality  $x_1 < x_2 < \dots < x_p$ . The method of images generates  $\frac{1}{2}p(p-1)$  negative walkers from the initial walker by reflection in each of the  $\frac{1}{2}p(p-1)$  wall planes. But for  $p > 2$  one must go on to consider the positive images of all these negative walkers, and so on, recursively. One discovers that the procedure *closes* after the generation of  $p!$  compound walkers, where each compound walker generated by a permutation  $\hat{\pi}$  of even parity,  $|\hat{\pi}|$ , is a normal, positive walker, while each walker corresponding to an odd permutation is a negative walker. Finally, therefore, if  $\hat{\pi}\vec{x}$  denotes the vector obtained from  $\vec{x}$  by permuting the coordinate labels, the overall distribution of  $p$  vicious walkers is given by

$$Q_n^{(p)}(\vec{x}, \vec{x}_0) = \sum_{\hat{\pi}} (-)^{|\hat{\pi}|} Q_n^0(\vec{x}, \hat{\pi}\vec{x}_0) \quad (5.9)$$

where  $Q_n^0(\vec{x}, \vec{x}_0)$  denotes the distribution for the appropriate free, compound walker in  $p$  dimensions: as indicated above, this is given asymptotically by (3.1) with  $\vec{x} \Rightarrow (\vec{x} - \vec{x}_0)$ .

From the master formula (5.9) all previously stated results follow. The antisymmetric character of the sum in (5.9) leads to a determinantal expression for the death factor which, in the case of walkers initially (or, finally) equispaced, reduces to a Vandermonde determinant. Such a determinant can be factorized and that yields the product formula (4.7). To obtain the result (4.15) for general initial and final spacing, the determinant elements,  $\exp(x_j x_{k,0}/b^2 n)$ , are expanded in powers of  $n^{-1}$  and a product of two Vandermonde determinants is obtained: details are given in Appendix A of Ref. 2.

### 5.4. Two Walkers and a Wall

The effectiveness of the method of images in complex cases depends upon the closure of the set of positive and negative images under all applicable reflections. This, in turn, requires some sort of underlying

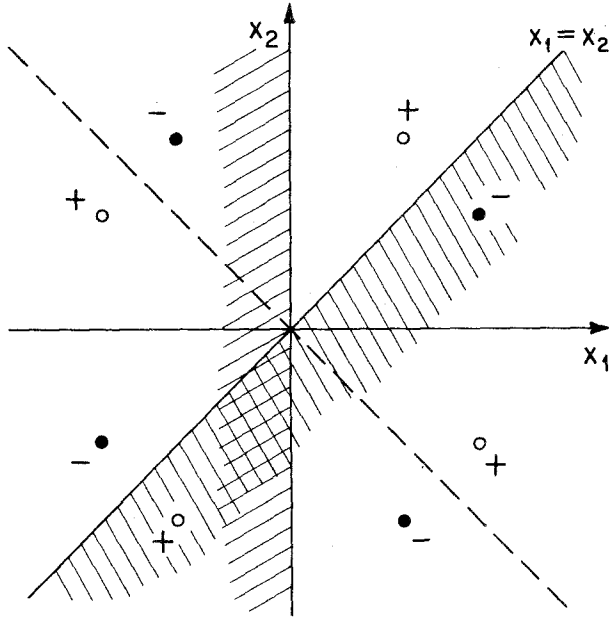


Fig. 5. The compound walker plane for two vicious walkers in the presence of an absorbing wall at  $x = 0$ . The constraints  $0 < x_1 < x_2$  yield two mirror planes,  $x_1 = 0$  and  $x_1 = x_2$ , which on reflection generate two more mirror planes, namely,  $x_2 = 0$  and  $x_1 = -x_2$ . As illustrated, a total of eight images, one being the original walker, result from the reflections.

symmetry in the system. Nevertheless a number of further problems can be discussed. In particular, an absorbing wall and two vicious walkers can be handled. As illustrated in Fig. 5 reflections in the two basic planes/lines determined by  $0 < x_1$  and by  $x_1 < x_2$  generate two further effective mirror planes but closure is obtained with eight images as shown. The probability of returns to fixed positions (near) the wall for large  $n$  are found to decay as

$$R_n^{W,2} = C_2^W/n^5 [1 + O(a^2/n)] \tag{5.10}$$

where the dependence on the initial and final coordinates is given by

$$C_2^W(\vec{x}, \vec{x}_0) = x_1 x_2 x_{1,0} x_{2,0} (x_2^2 - x_1^2)(x_{2,0}^2 - x_{1,0}^2)/3\pi \tag{5.11}$$

It is interesting that in this case, regarding the wall as just another walker (of low diffusivity) leads to wrong asymptotic behavior since, by (4.3), the probability of a reunion of  $p = 3$  vicious walkers varies as  $1/n^4$ : apparently the positional fluctuations of a third walk allow a slower decay than does a rigid wall.

### 5.5. Two Dissimilar Walkers

A direct application of the method of images to two *dissimilar* walkers fails because in the first section of a reflected walk the diffusivities,  $b_1^2$  and  $b_2^2$ , will necessarily be interchanged: but in the unreflected, second section of the walk interchanged diffusivities will cause the cancellation to fail, in general. This problem may, however, be tackled in the continuum model by separating variables via a change of coordinates to  $x = x_2 - x_1$  and  $\bar{x}$  as given by (4.19). The “mean” walker, with coordinate  $\bar{x}$ , diffuses freely; the “internal” walker is subject to  $x > 0$  but, as seen, that problem can be handled by the method of images. Combining the results yields (4.18).

### 5.6. Other Aspects

The basic expression (5.9) can be manipulated to yield further intriguing expressions describing the asymptotic behavior of  $p$  vicious walkers. It would clearly be of interest to obtain comparable exact results in which the limit  $p \rightarrow \infty$  could be taken maintaining, say, a constant density of walkers. Such results do, in fact, exist and we will make contact with some of them below. However, rather different and more elaborate forms of analysis seem called for. The antisymmetric character of the problem evident in (5.9) can be utilized to construct a representation in which walkers appear as quantum-mechanical particles moving (or “hopping”) in one dimension and collectively obeying Fermi statistics. Standard quantum-statistical methods for discussing free fermions then yield valuable exact results. One of the earliest studies along such lines was presented as a model for fibrous structures by de Gennes<sup>(4)</sup> in 1968. To pursue that theme here would, however, take us too far afield. Instead, let us turn now to some applications of the simple random walk results we have obtained.

## 6. PHASE TRANSITIONS IN LINEAR SYSTEMS

This section might have been headed “*Phase transitions with short range forces in one dimension (almost).*” Without the final qualifier, “almost,” this title would contradict many theorems that prove rigorously that one-dimensional statistical mechanical systems with short range forces (of finitely-many-body character) *cannot* exhibit *any* phase transitions at non-zero temperatures. However, systems which are “almost one-dimensional” in the sense that they have a dominant linear structure but can, in some sense, spread indefinitely in a transverse dimension, may well have phase transitions at positive temperatures even if only short-range forces are entailed: and, of course, truly one-dimensional systems with forces of

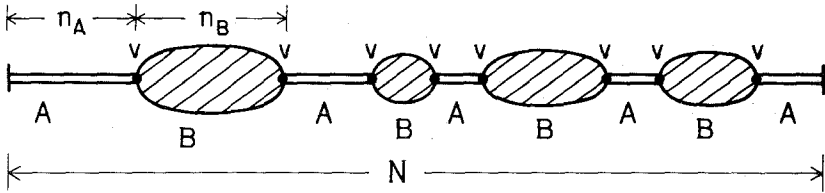


Fig. 6. Illustrating a linear system in the form of a necklace or string of total length  $N$  units made up of alternating segments of microstates  $A$  and microstates  $B$  (constituting “beads” or “bubbles”).

sufficiently long range most certainly exhibit phase transitions.<sup>7</sup> Furthermore even one-dimensional systems with interactions of short range can have transitions if many-body forces of indefinitely high order are allowed.<sup>8</sup>

In fact, there is a rather simple but general mathematical mechanism which underlies a broad class of *exactly soluble* one-dimensional models which display phase transitions. This mechanism does not seem to be as well appreciated as it merits and it operates in a number of the applications we wish to discuss. Accordingly it seems appropriate to present a brief exposition here.

Consider the necklace or string illustrated in Fig. 6 which consists of alternating segments, the first containing only a class of microstates labelled  $A$  of length  $n_A$  discrete units, and the second, only states of a class labelled  $B$  (for “bubble” or “bead”) of  $n_B$  units. If  $Z_N(T)$  is the partition function for such a necklace of total length  $N$  units, which represents a sum over all possible numbers and lengths of  $A$  segments and  $B$  segments, we require the *reduced free energy* per unit of length, namely,

$$f(T) = \lim_{N \rightarrow \infty} \frac{F_N}{Nk_B T} = - \lim_{N \rightarrow \infty} \frac{1}{N} \ln Z_N(T) = \Sigma/k_B T \quad (6.1)$$

where  $\Sigma(T)$  can be interpreted literally as the *tension* of the string.

An effective way to calculate  $f$  is to construct the isobaric partition function or generating function

$$G(z, T) = \sum_{N=0}^{\infty} z^N Z_N(T) \quad (6.2)$$

in which the activity-like variable  $z$  evidently acts as an indicator or counting variable for overall length. Then, if  $z_0(T)$  is the *positive real*

<sup>7</sup> Recall, for example, the renowned work of Dyson<sup>(5)</sup> on the one-dimensional Ising model with long-range forces; see also the recent results of Fröhlich and Spencer.<sup>(6)</sup>

<sup>8</sup> This is demonstrated in Refs. 7 and 8, which are of particular relevance in the present context.

singularity of  $G(z)$  lying closest to the origin, the limiting free energy is given simply by

$$z_0 = e^f \quad \text{or} \quad f(T) = \ln z_0(T) \quad (6.3)$$

This follows since  $Z_N$  is real and positive for all  $N$ , so that  $z_0$  determines the radius of convergence of the series (6.2). It is important to note that the singularity of  $G(z)$  at  $z_0$  may correspond to a divergence such as a simple pole  $\sim 1/(z_0 - z)$ , but may equally represent a nonanalyticity, such as a square root branch point, at which  $G(z)$  remains finite when  $z \rightarrow z_0 -$ .

So much is quite general; the power of the generating function approach is that for a necklace such as shown in Fig. 6,  $G(z)$  can be constructed explicitly in terms of the partial isobaric partition functions

$$G_A(z) = \sum_n Q_n^A z^n \quad \text{and} \quad G_B(z) = \sum_n Q_n^B z^n \quad (6.4)$$

Here  $Q_n^A(T)$  and  $Q_n^B(T)$  are the (canonical) partition functions for segments of length  $n$  of  $A$  states and  $B$  states, respectively. In fact a little thought shows<sup>9</sup> that one has

$$G(z) = G_A + G_A v G_B v G_A + G_A v G_B v G_A v G_B v G_A + \cdots \quad (6.5)$$

where successive terms correspond to segment sequences,  $A$ ,  $ABA$ ,  $ABABA$ , etc. and, for simplicity we have decreed that a necklace should always start and end with an  $A$  segment (a convention of no consequence in the thermodynamic limit if  ${}^9v \neq 0$ ). In addition we have introduced a *vertex weight* (or activity)  $v$  which can be regarded as a Boltzmann factor associated with each  $AB$  or  $BA$  junction. Now for sufficiently small  $z$  the expression (6.5) is simply a convergent geometric progression: thus we finally obtain

$$G(z) = G_A(z) / [1 - v^2 G_A(z) G_B(z)] \quad (6.6)$$

It is not hard to generalize this formula to describe a necklace with further types of bead  $CD \cdots$  arranged in periodic or arbitrary order, etc.

The possible mechanism for a phase transition is now already manifest. Thus,  $z_0(T)$ , the required singularity of  $G(z)$ , may be *either* the smallest root of the equation

$$v^2 G_B(z) = 1 / G_A(z) \quad (6.7)$$

or the closest real, positive singularity of  $G_A(z)$  or of  $G_B(z)$ : then, as the temperature or other parameters change, the condition determining  $z_0(T)$  and, thence  $f(T)$ , may *switch*; such a switch will, in general, be nonanalytic and hence must correspond to a phase transition.

<sup>9</sup> See, e.g., Refs. 2, 3, 7, and 8 and work of Temperley<sup>(9)</sup> which contains a variety of instructive examples. To include the limit  $v \rightarrow 0$ , it is useful to include also the sequences  $B, BAB, \dots$  so that the numerator in (6.6) becomes  $G_A(z) + G_B(z)$ .

To investigate this in the simplest nontrivial situation suppose that the  $A$  states are described merely by

$$A: \quad Q_n^A = u^n \quad \text{with, say,} \quad u = e^{-\epsilon/k_B T} \quad (6.8)$$

so that  $u$  increases as  $T$  increases, and the generating function is

$$G_A(z) = 1/(1 - uz) \quad (6.9)$$

This has a pole at  $z_A = 1/u$ ; however, it is easy to see from (6.6) that the denominator of  $G(z)$  must vanish *before*  $G(z)$  diverges at  $z_A$  so that this singularity never determines  $z_0$ .

For the  $B$  states we suppose that the canonical partition function for large  $n$ , which will be all that matters as regards the nature of any phase transitions, behaves as

$$B: \quad Q_n^B \approx q_0 w^n / n^\psi \quad \text{with} \quad w = e^{-\sigma_0(T)} \quad (6.10)$$

This is a rather natural generalization of (6.8) but its appropriateness will become quite clear when we consider various applications. Notice that the reduced free energy per unit length of a long bead or bubble is given simply by  $f = \sigma_0(T)$ . Now the behavior of the corresponding generating function as  $wz \rightarrow 1 -$  is easily estimated with the aid of the binomial theorem which yields

$$\begin{aligned} G_B(z) &\approx G_s / (1 - wz)^{1-\psi}, & \text{for } \psi < 1 \\ &\approx G_s \ln(1 - wz)^{-1} & \text{for } \psi = 1 \\ &\approx G_c - G_s(1 - wz)^{\psi-1} + G_1(1 - wz) + \dots, & \text{for } \psi > 1 \end{aligned} \quad (6.11)$$

where  $G_s$ , the amplitude of the leading singularity, which occurs at  $z_B = w^{-1}$ , is positive, as is

$$G_c = \sum_n Q_n^B / w^n < \infty \quad (\psi > 1) \quad (6.12)$$

When  $\psi$  is an integer ( $\geq 2$ ) the term  $G_s(1 - wz)^{\psi-1}$  gains a factor  $\ln(1 - wz)^{-1}$ . (Notice, also, that for  $\psi > 3$  further analytic terms dominate.)

Now notice that  $\hat{G}_B(z)$  *diverges* at  $z_B$  when (a)  $\psi \leq 1$ . Then, as explained for  $G_A$ , the denominator of  $G$  must vanish *before*  $z$  reaches  $z_B$ . Consequently, the free energy is *always* given by the smallest root of (6.7): this varies analytically with  $u, v$ , etc. so there can be *no phase transition*. On the other hand, when (b)  $\psi > 1$  it is not hard to see from Fig. 7 that the root  $z_0(T)$  will stick at  $z_0 = z_B = 1/w$  for small  $u$ , provided  $v^2 G_c < 1$ , but will switch to the smallest root of (6.7) when  $u$  exceeds the critical value

$$u_c = w(1 - v^2 G_c) \quad (6.13)$$

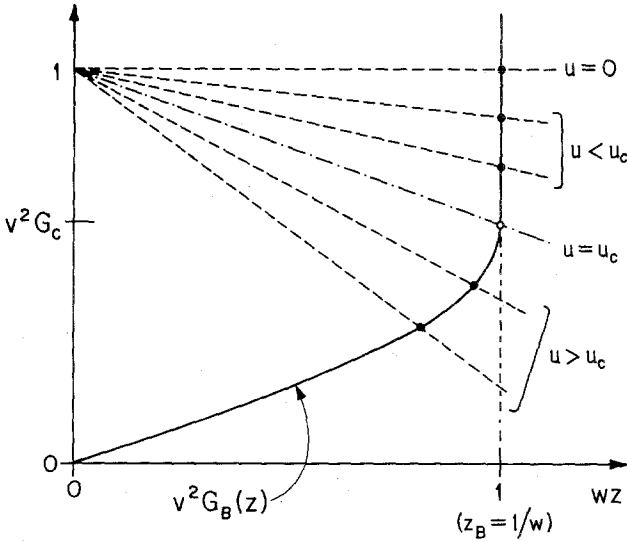


Fig. 7. Plot versus  $wz$  of  $v^2 G_B(z)$ , which remains finite but becomes singular at  $z = z_B = 1/w$  when  $\psi > 1$ . The dashed lines represent  $1/G_A(z) = 1 - uz$ . By (6.7) the circles locate the singularity,  $z_0(T)$ , which thus sticks at  $z = z_B$  for  $u < u_c$ .

The free energy *below*  $u_c$  is thus given simply by

$$f = \sigma_0(T) \quad (\text{all } \psi > 1) \tag{6.14}$$

which describes a “frozen” phase consisting, essentially, of one infinitely long bubble, i.e., only *B* states are realized in the thermodynamic limit. Above  $u_c$ , if one measures the deviation from the transition by

$$t = (T - T_c)/T_c \sim u - u_c \tag{6.15}$$

one finds *critical behavior*,

$$f = \sigma_0(T) - A_s t^{1/(\psi-1)} + \dots, \quad \text{for } 1 < \psi < 2 \tag{6.16}$$

with a logarithmic factor at  $\psi = 2$ , but a *first-order transition* plus singular corrections,

$$f = \sigma_0(T) - A_1 t + A_s t^{\psi-1} \dots, \quad \text{for } \psi > 2 \tag{6.17}$$

(Logarithmic factors in  $t$  appear in the corrections when  $\psi$  is integral and further terms,  $A_2 t^2, \dots$  dominate when  $\psi > 3$ .) The critical behavior (6.16) corresponds to a specific heat singularity with exponent<sup>(10)</sup>

$$\alpha = (2\psi - 3)/(\psi - 1) \tag{6.18}$$

The mean length of a given bubble in the “melted” or “disordered” phase can be calculated from

$$\bar{n}_B = z \frac{\partial}{\partial z} \ln G_B(z) \tag{6.19}$$

which, on using (6.16) for  $1 < \psi < 2$ , yields

$$\bar{n}_B \sim \frac{1}{(1 - wz)^{2-\psi}} \sim \frac{1}{(\sigma_0 - f)^{2-\psi}} \sim \frac{1}{t^{(2-\psi)/(\psi-1)}} \tag{6.20}$$

Not surprisingly, this diverges as  $t \rightarrow 0$ . On the other hand,  $\bar{n}_B$  remains finite at the first-order transition when  $\psi > 2$ . When the transition is critical one should expect to find a divergent, *longitudinal correlation length*,  $\xi_{\parallel}(T)$ . Its magnitude will be set by the average bubble length,  $\langle \bar{n}_B \rangle$ ; however, longer bubbles occupy more space on the necklace and so must be weighted accordingly in computing the average. Thus, if  $c$  is the length of a unit, we have

$$\begin{aligned} \xi_{\parallel} &= c \langle \bar{n}_B \rangle = c \overline{n_B^2} / \bar{n}_B = (c / \bar{n}_B) \left( z \frac{\partial}{\partial z} \right)^2 \ln G_B(z) \\ &\sim \frac{c}{1 - wz} \sim \frac{c}{\sigma_0 - f} \sim \frac{c}{t^{\nu_{\parallel}}} \end{aligned} \tag{6.21}$$

where the correlation length exponent is seen to be

$$\nu_{\parallel} = 1/(\psi - 1) \tag{6.22}$$

Comparison with (6.16) and (6.18) shows that this satisfies the standard hyperscaling relation,  $d\nu_{\parallel} = 2 - \alpha$ , with  $d = 1$ , in accord with normal expectations.<sup>(10,11)</sup>

Armed with this general formalism and the results for vicious walkers, let us, finally, turn to some concrete applications.

### 7. WETTING OF A BOUNDARY WALL IN TWO DIMENSIONS

Consider a system in thermodynamic equilibrium in a phase  $A$  which is on the point of a bulk first-order transition at which coexistence of the phase  $A$  with a second phase,  $B$ , becomes possible. Now if a wall of the container enclosing the bulk  $A$  phase becomes sufficiently attractive to the complementary phase,  $B$ , as, say,  $T$  increases, we may expect to see a *wetting transition*.<sup>(12,13)</sup> At such a transition the amount of  $B$ -like material adsorbed on the wall, or the mean thickness,  $l_w$  of the adsorbed,  $B$ -like film becomes *infinite* so that, the wall is, in fact, covered by a *macroscopically thick wetting layer* of bulk phase  $B$ ; this is separated from the bulk  $A$  phase by a normal  $A|B$  interface with surface tension

$$\Sigma_{AB}(T) = k_B T \sigma \tag{7.1}$$

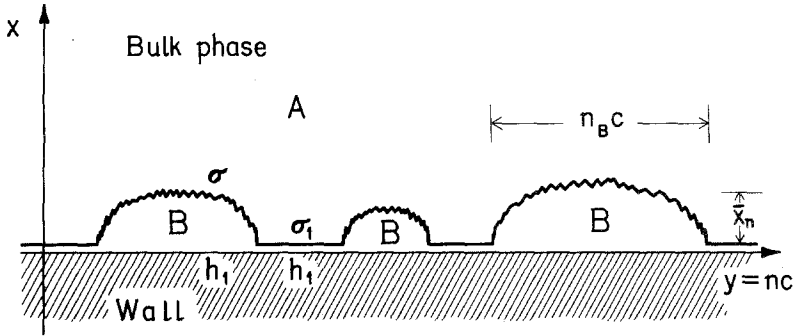


Fig. 8. Model of a prewetting layer on a wall in a two-dimensional system close to coexistence between bulk phases  $A$  and  $B$ . The reduced tensions  $\sigma$  and  $\sigma_1$  characterize a free interface and one pinned to the wall, respectively, while  $h_1$  is a local field or chemical potential favoring the  $B$  phase.

To model such a system we suppose, following Abraham,<sup>(14)</sup> that the wall affects the bulk interactions locally so that an interface located close to the wall has a modified interfacial tension,  $\Sigma_{AB}^{(1)} = k_B T \sigma_1$ . If, as we suppose,  $\Sigma_{AB}^{(1)} < \Sigma_{AB}$  holds for low  $T$ , the interface tends to be pinned to the wall. One may similarly represent the specific attraction of the wall for the phase  $B$  by a local field or (reduced) chemical potential,  $h_1$ , although this parameter plays no essential role in the present case. Abraham<sup>(14)</sup> solved this problem<sup>10</sup> *exactly* for a ( $d = 2$ )-dimensional Ising model and, indeed, discovered a wetting transition at a temperature  $T_W$ , below the bulk critical point,  $T_c$ . We will solve a simplified version of Abraham's model or, to express it differently, solve his model approximately by heuristic arguments which prove, however, good enough to capture the principal results *exactly*!<sup>11</sup>

Our model or "picture" of a wall in a two-dimensional system below the wetting transition is embodied in Fig. 8. The interface is pinned to the wall along segments of varying length but escapes from the wall over alternate segments to form bubbles or droplets of  $B$  phase bounded by

<sup>10</sup> Abraham<sup>(14)</sup> described the phenomenon as an interface *roughening transition*<sup>(15)</sup> since the unbound interface above  $T_W$  is, in fact, rough: however, since a *free* interface in two dimensions is *always* rough it was recognized later that the transition in Abraham's model is primarily a wetting or *interface delocalization* transition: see also Chui and Weeks.<sup>(16)</sup>

<sup>11</sup> Other treatments of versions of the simplified model have been given by Chui and Weeks,<sup>(16)</sup> by Burkhardt,<sup>(17)</sup> and by van Leeuwen and Hilhorst.<sup>(18)</sup> However, these authors have used somewhat more elaborate approaches based on the Schrödinger-like diffusion equation for a walk in a potential which is discussed below.

sections of  $A|B$  interface. The fluctuations of the interface normal to the wall, which we take to be the  $x$  direction, are modeled by a random walk for which the  $y$  coordinate, parallel to the wall, represents time, i.e., we take  $y \equiv t = nc$ . In this picture “overhangs” or “double-backs” are disregarded as in the original Temperley<sup>(19)</sup> or solid-on-solid (SOS) model<sup>(16)</sup> of a  $d = 2$  Ising model interface. In a long, free, statistically straight interface, overhangs can certainly be absorbed into a fully renormalized value of the interfacial tension: however, it is not easy to assess directly whether the neglect of overhangs is of any greater significance in curved and restricted interfaces of finite, albeit long length such as entailed in bubbles on a wall.

As clear from Fig. 8, our model is just a special type of *necklace* of the sort discussed in the previous section. The interaction parameters are to be identified as

$$u = e^{-\sigma_1 + h_1} \quad \text{and} \quad w = e^{-\sigma + h_1} \quad (7.2)$$

The vertex weight may, for present purposes, be absorbed into the prefactor  $q_0$  in (6.10). The all-important exponent  $\psi$  follows from our analysis of a walk near an absorbing wall: to this end, recall from (5.6) that the number of  $n$ -step returns to the wall,  $R_n^W$ , decays as  $1/n^{3/2}$ . Hence we have

$$\psi = 3/2 \quad (7.3)$$

The results can now be read off from (6.14) to (6.20). As the tension,  $\Sigma_{AB}(T)$ , of a free interface decreases with increasing  $T$  bubbles of greater and greater length appear and the wall free energy or, equivalently, the modified interfacial tension finally exhibits a transition where it varies as<sup>(2,20)</sup>

$$\begin{aligned} f \equiv \Sigma_W/k_B T &= \sigma(T) - A_0(T - T_{cW})^2 + \dots, & \text{for } T \leq T_{cW} \\ &= \sigma(T), & \text{for } T \geq T_{cW} \end{aligned} \quad (7.4)$$

Evidently this wetting transition is critical and, indeed, corresponds precisely to a classical second-order transition with a simple discontinuity in the specific heat ( $\alpha = 0$ ); see also Fig. 9. This result agrees precisely with the exact Ising model calculations of Abraham!<sup>(14)</sup> For  $T$  above the transition the equality  $f = \sigma$  shows that one has a free interface uninfluenced by the wall so that  $l_W(T) = \infty$ ; i.e., the wall is *completely wet*.

The longitudinal correlation length,  $\xi_{\parallel}(T)$ , describing density or composition correlations parallel to the wall below  $T_{cW}$ , now diverges with exponent  $\nu_{\parallel} = 2$  [see (6.22)]. Physically, it is also interesting to investigate the *transverse correlation length*,  $\xi_{\perp}(T)$ , describing correlations normal to the wall, and to determine the rate of divergence of the adsorption or,

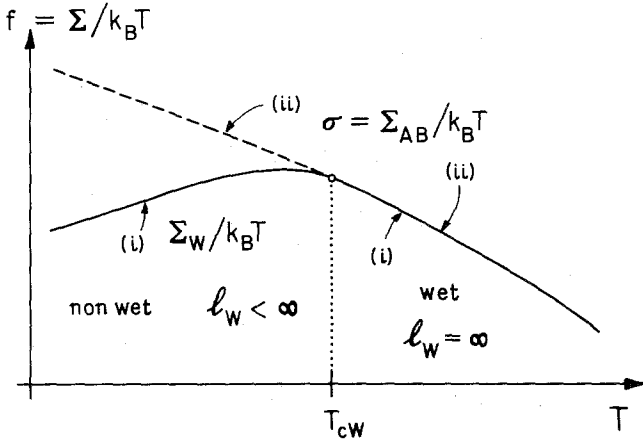


Fig. 9. Schematic variation (i) of the wall free energy,  $\Sigma_W(T)$ , (or wall-modified tension) through a critical wetting transition in a two-dimensional system. The tension  $\Sigma_{AB}$  of a free  $A|B$  interface, (ii), is approached quadratically as  $T$  approaches  $T_{cW}$  from below, while the thickness,  $l_W$ , of the adsorbed film, diverges as  $1/(T_{cW} - T)$ .

equivalently, the mean thickness  $l_W$  of the microscopic film of  $B$ -like phase. To do this let us examine the characteristic:

**7.1. Size and Shape of a Droplet on a Wall.** Accordingly, in a bubble of length  $nc$  consider the displacement,  $x$ , of the interface from the wall at a distance  $mc$  from one end of the bubble. The interfacial segments of  $m$  steps and  $(n - m)$  steps, respectively, may be described by *independent* walks from a point at a small distance,  $a$ , from the wall to the point  $x$ . From (5.5) the distribution of  $x$  for large  $m$  and  $n$  is thus proportional to

$$Q_m^W(x) Q_{n-m}^W(x) \propto a^2 x^2 \exp\left(-\frac{x^2}{2b^2 m} - \frac{x^2}{2b^2(n-m)}\right) \quad (7.5)$$

From this the mean value of  $x$ , the dispersion in  $x$ , etc. are readily calculated. These all scale with the most probable value of  $x$ . If the origin for  $y$  is taken at the midpoint of the bubble, so that  $m = \frac{1}{2}n + (y/c)$ , this is readily found to obey

$$x^2 + (2b^2/nc^2)y^2 = \frac{1}{2}nb^2 \quad (7.6)$$

Hence the bubble is, on average, *elliptical in shape!* Furthermore the mean area and width are given by

$$\bar{A}_n \approx \frac{\pi bc}{4\sqrt{2}} n^{3/2} \quad \text{and} \quad \bar{x}_n \approx \frac{\pi b}{4\sqrt{2}} n^{1/2} \quad (7.7)$$

Of course the exponents here could have been guessed easily since the spread of a random walk of  $n$  steps is always of order  $bn^{\frac{1}{2}}$ .

With this information we can estimate the transverse correlation length and the adsorption.<sup>(2,3)</sup> For the former we have

$$\begin{aligned} \xi_{\perp} &\approx \langle \bar{x}_n \rangle \sim b \langle \bar{n}_B^{-\frac{1}{2}} \rangle \sim b \bar{n}_B^{3/2} / \bar{n}_B \sim b / (1 - wz)^{\frac{1}{2}} \\ &\sim b (\xi_{\parallel} / c)^{\frac{1}{2}} \sim b / t^{\nu_{\perp}} \quad \text{or} \quad \nu_{\perp} = \frac{1}{2} \nu_{\parallel} \end{aligned} \quad (7.8)$$

so that  $\nu_{\perp} = 1$ . The adsorption follows similarly<sup>(2)</sup> as

$$\rho_B \propto \langle \bar{A}_n \rangle / \langle \bar{n}_B \rangle \sim \bar{n}_B^{5/2} / \bar{n}_B^2 \sim (1 - wz)^{-\frac{1}{2}} \sim \xi_{\perp} \quad (7.9)$$

and hence diverges in the same way as the transverse correlation length, as is physically reasonable. The mean *thickness*,  $l_w(T)$ , of the prewetting film can equally be regarded as measured by  $\xi_{\perp}$ .

**7.2. Interface Pinning in the Bulk.** We have seen above that if an interface is attracted to a wall it may be pinned at the wall but can then break loose, or “delocalize,” at a wetting transition at some  $T = T_{cW}$ . [To check that the transition does actually occur in a given model it is necessary to pay a little more attention to the vertex weight,  $v$ , than we did above and, in particular, to verify that the transition point given by (6.13) actually falls within the physical region; e.g.,  $T_{cW}$  should be less than the bulk critical point  $T_c$ .] It is natural to enquire further whether an interface in a *bulk* two-dimensional system can be similarly pinned by a *linear imperfection*, (away from any walls) and then undergo a *depinning* or *delocalization transition*.<sup>(16–18)</sup> To be concrete, consider a nearest-neighbor ferromagnetic square lattice Ising model with a row parallel to the  $y$  axis (i.e., “horizontal” in the presentation of Fig. 8) of weakened  $x$  bonds (“vertical” bonds in Fig. 8). An interface parallel to the  $y$  axis will, clearly, be pinned on the row of weakened bonds at  $T = 0$ , since the interfacial tension will be lowest there. As  $T$  increases, however, segments of the interface may break loose, wander on *either side* of the attractive row of bonds, and then return to form a pinned segment. Since the interface may wander *across* the attractive row without actually experiencing the pinning potential its behavior may, in essence, be described just by the returns of a free walker. By (2.7) we thus have  $\psi = \frac{1}{2}$  and hence, by the analysis following (6.12), there is *no transition*: in other words the interface *always remains pinned* however weak the attractive row potential! This conclusion is confirmed, again, by the more elaborate arguments.<sup>(16–18)</sup>

## 8. MULTIPHASE SYSTEMS: INTERFACIAL WETTING

### 8.1. Two-Dimensional Fluids

Consider a multiphase two-dimensional system in which three or more different phases  $A, B, C, \dots$  can coexist. Between these phases various distinct interfaces may be formed. Then, as one varies the temperature or composition, etc., one of these interfaces, say  $A \parallel C$ , may undergo a wetting transition, becoming wet by an "intermediate phase," say,  $B$ , and decomposing into an  $A \parallel B$  interface and a separate  $B \parallel C$  interface, as illustrated schematically in Fig. 10. Indeed current experiments on three-dimensional systems are performed on such multiphase fluid systems in which, typically,  $A$  is vapor phase.<sup>(21-24)</sup> The analogous experiments on multicomponent adsorbed fluid films should be possible.

Now if, as before, we model the various interfaces by random walks we see from Fig. 10 that an intact  $A \parallel C$  interface may be regarded as a necklace of segments, say, "threads," in which the local composition profile changes rapidly with  $x$  from bulk  $A$ -like to bulk  $C$ -like, and "bubbles" describing regions where a sliver of intermediate,  $B$ -like phase penetrates as a fluctuation. The former segments may be described by a reduced "bare"

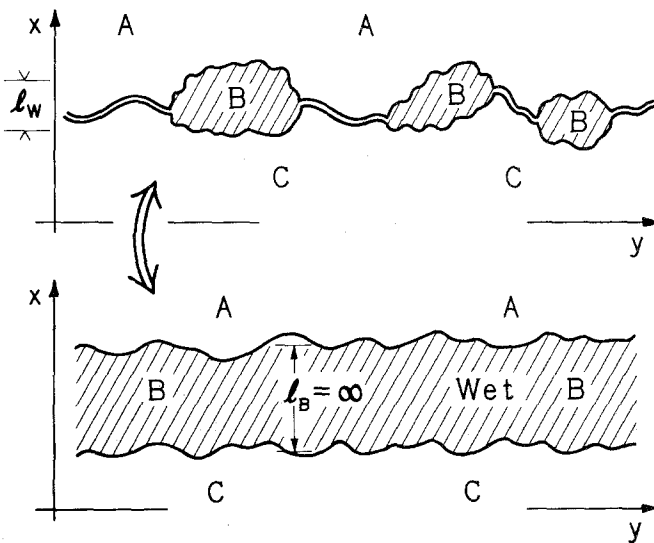


Fig. 10. Illustration of an interfacial wetting transition in a two-dimensional three-phase system. The free  $A \parallel C$  interface has fluctuations in which microscopic droplets of  $B$ -like phase appear on the interface. When these grow and coalesce the  $A \parallel C$  interface can decompose into distinct  $A \parallel B$  and  $B \parallel C$  interfaces separated by a macroscopic wetting layer of  $B$  phase.

or “local” tension,  $\sigma_{AC}$ , while the latter, consisting essentially of two distinct, more-or-less parallel interfaces can be described by a total reduced tension  $\sigma_{AB} + \sigma_{BC}$  where

$$\sigma_{AB} = \Sigma_{AB}/k_B T \quad \text{and} \quad \sigma_{BC} = \Sigma_{BC}/k_B T \quad (8.1)$$

in which  $\Sigma_{AB}(T)$  and  $\Sigma_{BC}(T)$  are the tensions of free, well-separated  $A|B$  and  $B|C$  interfaces. The necklace parameters may then be taken as

$$u = e^{-\sigma_{AC}} \quad \text{and} \quad w = e^{-\sigma_{AB} - \sigma_{BC}} \quad (8.2)$$

while the vertex activity,  $v$ , can be used to allow for the deviations of the total bubble tension from  $\sigma_{AB} + \sigma_{BC}$  induced by the two sides of the bubble coming together at the vertex.

Finally, the exponent  $\psi$  now required is that associated with the reunion of  $p = 2$  vicious walkers so that by (4.4) we have

$$\psi = 3/2 \quad (8.3)$$

This is the *same* as for the wetting of a rigid wall in a two-phase system. Thus the wetting transition will again be critical with classical, second-order exponents. In particular, the surface tension of the intact, nonwet  $A||C$  interface varies when  $T$  approaches  $T_{cW}$ , say, from below, as

$$\Sigma_{AC}(T) = \Sigma_{AB}(T) + \Sigma_{BC}(T) - A_0(T - T_{cW})^2 + \dots \quad (8.4)$$

while in the wet region,  $T > T_{cW}$ , one has simply

$$\Sigma_{AC}(T) = \Sigma_{AB}(T) + \Sigma_{BC}(T) \quad (8.5)$$

This represents Antonow’s rule<sup>(25)</sup> for the situation in hand and, clearly, describes two well-separated interfaces with a wetting layer of macroscopic thickness between them, i.e.,  $l_B = \infty$  (see Fig. 10). Graphically, Fig. 9 still applies with the curve (i) representing the tension  $\Sigma_{AC}(T)$ , while curve (ii) represents the sum  $\Sigma_{AB} + \Sigma_{BC}$ . The longitudinal and transverse correlation length exponents and the exponent for the adsorption of  $B$ -like material on the  $A||C$  interface must all be the same as found in the previous section.

Notice that in quoting (4.4) as authority for  $\psi = 3/2$  we were implicitly assuming that the two distinct interfaces  $A|B$  and  $B|C$  could be modeled by *similar* random walks. In general, the  $A|B$  and  $B|C$  interfaces will be physically *dissimilar* so this is not a satisfactory approximation. Nevertheless, as we have seen in Section 5, the reunions of two dissimilar walkers are, equally, described by  $\psi = 3/2$  so that (8.3) remains valid. This fact also makes it clear why the wetting of a rigid wall exhibits the same critical behavior.

## 8.2. Denaturation of a Biopolymer

The upper part of Fig. 10 may be regarded as a portrayal of a double-stranded biopolymer molecule, such as DNA, in which, over some segments, the two strands have become unwound from one another. Once the unwinding encompasses the whole length of the polymer molecule it dissociates into two separate chains, corresponding schematically to the "wet" arrangement of interfaces in the lower half of Fig. 10. The accompanying transition in a long biopolymer molecule may be very sharp:<sup>12</sup> it is generally referred to as the helix-coil ( $A \equiv$  "helix,"  $B \equiv$  "coil" in the necklace picture), denaturation, or, simply, "melting" transition.

This transition can be discussed on the basis of the necklace theory<sup>(26)</sup> and one discovers that the sharpness of the transition is directly related to the smallness of the vertex activity,  $v$ , which in this context is sometimes called the "initiation factor." The exponent  $\psi$  enables one to account for the self-avoiding character of the two, partially dissociated, "coiled" strands of polymer which constitute a necklace bubble.<sup>(28)</sup> The necklace theory does not, however, take account of the self-avoiding or "excluded volume" requirement between different bubbles or between bubbles and bound, "helical" segments. To correct this deficiency represents a very difficult problem but one may hope it is not too serious in the case that the helical sections are comparatively rigid, as is so in most real situations.

## 8.3. Commensurate Adsorbed Phases

When submonolayers of an atomic or simple molecular gas are adsorbed on smooth crystalline substrates one frequently observes (by x-ray and electron scattering techniques) the formation of *commensurate surface phases* in which the adsorbate atoms are, predominantly, ordered in registry with the underlying substrate lattice. Such phases may be formed and studied under conditions of thermodynamic equilibrium. Then, as the temperature,  $T$ , and chemical potential,  $\mu$  (which controls the overall adsorbate coverage), are varied the degree of order changes and the commensurate phase may melt into a disordered, fluid phase, or undergo a transition into a different commensurate phase or into an incommensurate phase.<sup>13</sup>

The simplest type of commensurate phases to study are the uniaxial  $p \times 1$  phases in which, on a substrate of rectangular symmetry, the adsorbate atoms define a superlattice in which the  $x$ -axis lattice constant is an

<sup>12</sup> See the review and reprint collection by Poland and Scheraga<sup>(26)</sup> and, for example, Stevens and Felsenfeld.<sup>(27)</sup>

<sup>13</sup> See the collection of lectures edited by Dash and Ruvalds.<sup>(29)</sup>

integer,  $p$ , times the corresponding substrate lattice constant, say,  $a$ . In the ideal, fully ordered situation the adsorbate atoms (or molecules) will thus form uniformly spaced chains parallel to the  $y$  axis and at distance  $pa$  apart. A physical realization of such  $p \times 1$  rectangular phases for  $p = 1, 2,$  and  $3$  is formed by dissociated, and hence atomic, hydrogen on the (110) face of crystalline iron<sup>(30)</sup> (although in the  $p = 3$  phase it is chains of vacancies rather than of atoms which are separated by three lattice spacings).

Now it is evident that a  $p \times 1$  phase gives rise to  $p$  physically distinct but equivalent types of domain  $A, B, C, \dots$ . If different domains coexist on the substrate they must be separated by domain walls or interfaces where there is a mismatch in the ordering. However, even though all domains are completely equivalent, there will, as has recently been stressed,<sup>(2,3,20)</sup> be  $(p - 1)$ -distinct types of physically nonequivalent domain walls. This is evident from Fig. 11, which illustrates the case  $p = 4$  schematically. The types of wall or interface may be labeled by  $q$ , the discrete phase shift measured in units of the  $x$  lattice spacing which is generated on crossing the interface from one domain to its neighbor. Thus for  $p = 4$  we have the three types:

$$\begin{aligned}
 [+1] &\equiv [-3] & : & A|B, \quad B|C, \quad C|D, \quad \text{and} \quad D|A \\
 [+2] &\equiv [-2] & : & A||C, \quad B||D, \quad C||A, \quad \text{and} \quad D||B \\
 [+3] &\equiv [-1] & : & A|||D, \quad B|||A, \quad C|||B, \quad \text{and} \quad D|||C
 \end{aligned}
 \tag{8.5}$$

Each type of wall will have its own distinct free energy or tension,  $\Sigma_q(T, \mu)$ .

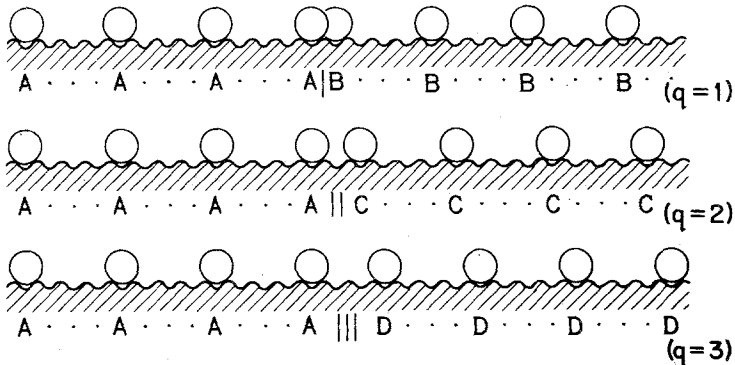


Fig. 11. Schematic cross-sections showing two contiguous domains of a  $p \times 1$  rectangular commensurate phase on a substrate when  $p = 4$  and demonstrating the existence of three physically distinct types of domain wall or interface with phase shifts  $q = 1, 2,$  and  $3$ . (See also Huse and Fisher, Refs. 2 and 20.)

Consider a  $p = 3$  phase. There are just two wall types:  $[+] \equiv [+1]$  and  $[-] \equiv [-1] \equiv [2]$ . As  $T$  and  $\mu$  vary, their tensions,  $\Sigma_+(T, \mu)$  and  $\Sigma_-(T, \mu)$ , will change and thus we may anticipate wetting transitions. Figure 10 would then represent the transition

$$[-] \Rightarrow 2[+], \quad \text{i.e.,} \quad A \parallel C \Rightarrow A | B | C \quad (8.7)$$

which will occur if  $2\Sigma_+(T, \mu)$  approaches  $\Sigma_-(T, \mu)$ . Our theory indicates that the transition should be continuous with classical, second-order thermodynamic exponents,  $\alpha = 0$ , etc., and correlation length exponents  $\nu_{\parallel} = 2$  and  $\nu_{\perp} = 1$ .

More generally, for  $p \geq 4$  one can have<sup>(2)</sup>

$$[-] \equiv [p-1] \Rightarrow (p-1)[+], \quad \text{e.g.,} \quad A \parallel\parallel D \Rightarrow A | B | C | D \quad (8.8)$$

To discuss this on the necklace picture we need  $\psi$  for  $q = (p-1)$ -stranded bubbles, which is described by the reunions of  $q$  vicious walkers. For  $q \geq 3$  we have  $\psi_q \geq 4$  and hence, by (6.17), we expect a *first-order transition* (although singular corrections will be present on the coherent, or intact, nonwet side of the transition). However, there are other possibilities for  $p \geq 4$ . Thus it may well happen that in one region of the phase diagram

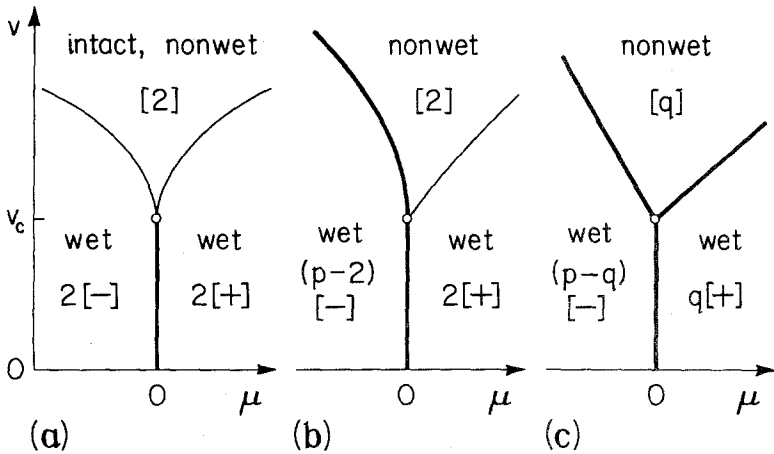


Fig. 12. Phase diagram for wet-to-wet domain wall transitions in  $p \times 1$  commensurate adsorbed phases for a  $[2]$  wall when (a)  $p = 4$  and (b)  $p \geq 5$ , and (c) for a  $[q \geq 3]$  wall with  $p - q \geq 3$ . First order transitions are denoted by bold lines; the light lines denote classical second-order transitions. An intact or coherent wall exists only for  $v > v_c$ . (After Huse and Fisher, Ref. 2.)

only  $[+]$  walls are stable, all other  $[q \neq 1]$  walls being wet, i.e., dissociated into  $(p - q)$   $[-]$  walls. This leads one to consider a necklace model in which both  $A$  and  $B$  segments are characterized by generating functions like (6.10) with (6.11) so that one has two exponents,  $\psi_A \equiv \psi_{p-q}$  and  $\psi_B \equiv \psi_q$ . The general theory still applies but it transpires that the vertex weight,  $v$ , plays a more important role. If  $v$  is less than a critical value

$$v_c = [G_c^{(p-q)} G_c^{(q)}]^{1/2} \quad (8.9)$$

[extending the notation of (6.11) and (6.12) in an obvious fashion] one always has a first-order, wet-to-wet transition, such as  $2[-] \Rightarrow 2[+]$  for  $p = 4$ . This is illustrated in Fig. 12, where the ordinate is  $v$  while the abscissa, labelled by the chemical potential, corresponds, precisely, to  $\mu = \sigma_- - \sigma_+$  where, in the general theory,  $w_A = e^{-\sigma_-}$  and  $w_B = e^{-\sigma_+}$ . As shown in the figure, the wetting transitions above  $v_c$  are normal (i.e., an intact, coherent wall dissociates) and may be either first order or second order in character, depending on the values of  $p$  and  $q$ . Consequently, the phase diagrams can exhibit a *bicritical point* from which spring two critical lines, a *critical endpoint*, or a *triple point*; see Fig. 12.

#### 8.4. Chiral Melting

There is good evidence, both theoretically and experimentally,<sup>14</sup> that the melting of a two-dimensional commensurate phase may be *continuous*. The question then arises as to the universality class of the transition or, more concretely, as to the values of the critical exponents. This issue has been reopened recently in light of the observations above concerning different types of domain wall.<sup>(2,20)</sup> Let us consider, specifically, a  $p \times 1$  commensurate adsorbed phase with  $p = 3$ : then there are just two types of wall, namely,

$$\begin{aligned} [+ ] & : A | B, \quad B | C, \quad \text{or} \quad C | A \\ [- ] & : A \parallel C, \quad B \parallel A, \quad \text{or} \quad C \parallel B \end{aligned} \quad (8.10)$$

Now a continuous melting transition implies the existence of large-scale fluctuations: but the important fluctuations in an initially fully ordered domain, say, an  $A$  domain, are those which can be represented as small subdomains of contrasting character, i.e.,  $B$  and  $C$ . Near criticality such subdomains will become large and, thus, their perimeters will resemble the domain walls  $[+]$  and  $[-]$ . The four simplest types of subdomain fluctuations are illustrated schematically in the upper left part of Fig. 13.

<sup>14</sup> See, e.g., Refs. 2, 20, and, experimentally, Bretz<sup>(31)</sup> and Moncton *et al.*<sup>(32)</sup>

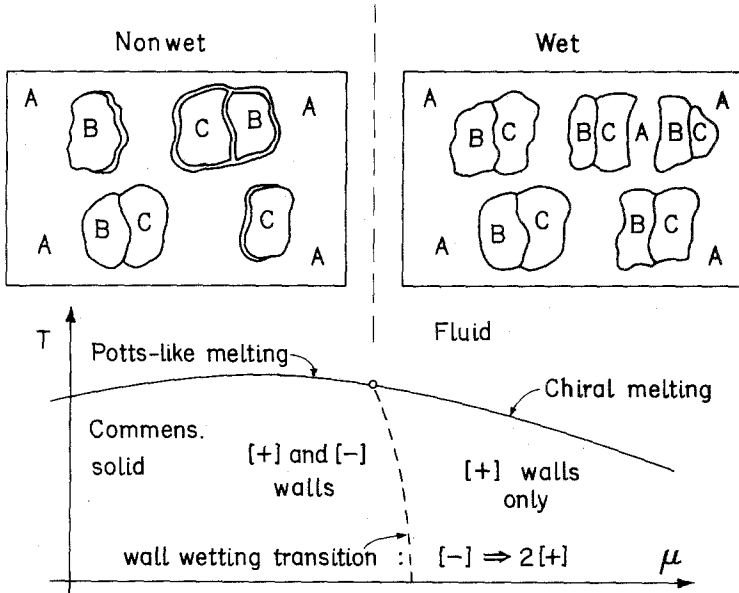


Fig. 13. Schematic depiction of the predominant heterophase subdomain fluctuations near a continuous commensurate melting transition when  $[-]$  walls are not wet, as on the left, or are wet, by the intermediate domain, as on the right. The corresponding (schematic) phase diagram exhibits a wall-wetting transition locus within the commensurate solid phase and a continuous melting line which changes from Potts-like to chiral character. Such a phase diagram may apply to  $\sqrt{3} \times \sqrt{3}$  commensurate phases as found in krypton on graphite; see Ref. 20.

This picture supposes, however, that both  $[+]$  and  $[-]$  walls remain intact, i.e., are *nonwet*. In this situation the critical fluctuations will resemble those in a two-dimensional ( $p = 3$ )-state *Potts model*. For nearest-neighbor coupling on a rectangular lattice this model can be described by the *clock model* Hamiltonian

$$\mathcal{H} = -J_x \sum_{\langle i,j \rangle}^{\perp} \cos \frac{2\pi}{p} (n_i - n_j) - J_y \sum_{\langle i,j \rangle}^{\parallel} \cos \frac{2\pi}{p} (n_i - n_j) \quad (8.11)$$

with  $p = 3$ . Here the first sum, labelled  $\perp$ , runs over nearest-neighbor pairs of transverse bonds, parallel to the  $x$  axis, while the second sum runs over longitudinal bonds, parallel to the  $y$  axis: the clock variables take the values  $n_i = 0, 1, 2, \dots, (p-1), [\text{mod } p]$ . In the ordered state of the clock and Potts models  $p$  physically equivalent types of domain exist just as in the  $p \times 1$  commensurate phases. Thus, in agreement with earlier considerations,<sup>(33,34)</sup> we are led to conclude<sup>(2,20)</sup> that if, as the phase boundary is approached,

both  $[+]$  and  $[-]$  walls remain intact, the continuous melting transition should be in the same universality class as the three-state Potts model. By this token the specific heat exponent should be  $\alpha = \frac{1}{3}$ , and so on. (In this connection we should recall Baxter's exact calculations for the melting of hard hexagons on a triangular lattice.<sup>(35,36)</sup> This transition is also expected to be in the  $p = 3$  Potts class and Baxter found  $\alpha = \frac{1}{3}$ .)

On the other hand, suppose that as the chemical pressure increases the  $[-]$  wall undergo a wetting transition and so decompose entirely into pairs of  $[+]$  walls. The phase diagram, see Fig. 13, now has a wetting line (shown dashed) and a region where any long  $[-]$  walls are unstable. Thus the previously identified set of simplest critical fluctuations will change character drastically as illustrated in the upper right part of Fig. 13: the most probable large fluctuations are now only  $A(B|C)A$  subdomains, the complementary or reflected  $A(C||B)A$  subdomains being suppressed. The configurational combinations of these fluctuations are unlike those of the three-state Potts model and thus, in contrast to the earlier considerations,<sup>(33,34)</sup> (which overlooked the lack of symmetry which allows different types of wall), we conclude<sup>(2,3,20)</sup> that continuous melting should be in a *new, chiral melting* universality class when only one type of wall remains intact as the phase boundary is approached.

The name "chiral" has been given to this new type of melting<sup>(2,20)</sup> to highlight the reflection noninvariance of the true adsorbate Hamiltonian that results in the two-domain configurations  $A|B|C$  and  $C||B||A$  having different free energies. In the standard Potts or clock models these two configurations are precisely equivalent and have the same free energy. At this point we do not know the details of chiral melting; in particular, the critical exponents have not been estimated reliably. However, the nature of the critical scattering in the disordered, fluid phase does provide an observable hallmark which distinguishes chiral from nonchiral continuous melting.<sup>(2,20)</sup>

## 8.5. Chiral Clock Models

To this point our discussion of domain wall wetting and commensurate melting has been quite phenomenological. One may reasonably doubt whether such wetting transitions will ever arise naturally in real systems or in sensible models and, even if they do, whether the difference in domain wall free energies, which is what ultimately drives the wetting transitions, will represent a *relevant perturbation*, in the renormalization group sense,<sup>15</sup> at the continuous melting transition.

<sup>15</sup> See, e.g., Refs. 70 and 11 and references therein.

The first issue can be answered physically by noticing from Fig. 11 that the different types of domain wall differ primarily in terms of the local density of the adsorbate atoms in the region of the wall<sup>(20)</sup>: if the adsorbate particles repel on close approach, a “heavy” or denser-than-average wall will have a higher free energy (or tension) than a “light” wall. In reaching this conclusion, however, the overall surface pressure, which is controlled by the chemical potential,  $\mu$ , has been overlooked. As  $\mu$  increases the coverage will increase above the ideal dictated by perfect registry with the substrate. The consequent “crowding” of the adsorbate will favor heavy walks reducing their free energy, say,  $\Sigma_+$ , relative to that of the light wall, say,  $\Sigma_-$ . Ultimately, this process can lead to an *incommensurate phase* (see further below): before this happens, however, the wetting condition  $2\Sigma_+ = \Sigma_-$  is likely to be encountered and the light, say,  $[-]$  walls will disappear.

A more concrete theoretical answer is provided by studying the so-called *chiral clock models* devised by Ostlund,<sup>(38)</sup> with this specific issue in mind, and, independently, by Huse.<sup>(39)</sup> These models allow for the chiral character of real adsorbed phases by, in the uniaxial case, generalizing the first term in the clock Hamiltonian (8.11) by supposing  $j$  always denotes the right-hand neighbor of  $i$  and taking

$$-J_x \sum_{\langle i,j \rangle}^{\perp} \cos \frac{2\pi}{p} (n_i - n_j + \Delta) \quad (8.12)$$

The parameter  $\Delta$  measures the degree of chirality; thus for  $p = 3$  the energy of the configurations  $\{n_i\} = \dots 012012 \dots$  of “spins” along the  $x$  axis, deviates from the energy of  $\{n_i\} = \dots 210210 \dots$  by a term proportional to  $\Delta$ . One may hence associate  $\Delta$  with the chemical potential  $\mu$ .

The chiral clock models can be studied by systematic series expansions at low and high temperatures.<sup>(3)</sup> In this way one discovers, first, that there are two distinct wall tensions obeying

$$\Sigma_+(T, \Delta) - \Sigma_-(T, \Delta) \approx -D(T)\Delta, \quad \text{as} \quad \Delta \rightarrow 0 \quad (8.13)$$

and second, that domain wall wetting transition lines,  $T_w(\Delta)$ , do, indeed, lie within the commensurate phase region,<sup>16</sup> resembling the behavior illustrated in Fig. 13 when  $T_w \rightarrow 0$ . Furthermore, one finds<sup>(3)</sup> for  $p = 3$  that at the pure Potts critical point, which is realized when  $\Delta \equiv 0$ , the chirality is a *relevant* perturbation so that for  $\Delta \neq 0$  the melting transition should cross over from Potts-like behavior and exhibit the anticipated new chiral character.

<sup>16</sup> As  $T \rightarrow 0$  the wetting lines for  $[-] \Rightarrow 2[+]$  and for  $[+] \Rightarrow 2[-]$  approach  $\Delta_w = \pm \frac{1}{4}$ , respectively, whereas the commensurate phase, represented at  $T = 0$  by  $n_i = 0$  (or 1 or 2) for all  $i$ , extends to  $\Delta_m = \pm \frac{1}{2}$ ; see Ref. 3.

### 9. THE FORCES BETWEEN WALKS AND WALLS

Studies of incommensurate phases in two and three dimensions have led various workers to the notion that parallel interfaces at separation  $l$  in a multiphase system act as if there were a well-defined force of interaction between them, at least for separations  $l \gg b$ , where  $b$  measures the intrinsic width of the interface.<sup>17</sup> This viewpoint has been particularly stressed by Pokrovsky,<sup>(40)</sup> by Villain,<sup>(41)</sup> and by Halperin and coworkers.<sup>(42)</sup> It can be extended to discuss the dependence of critical exponents on dimensionality regarded as a continuous parameter<sup>(43,44)</sup> and, as will be explained below, it can be used to discuss interfaces and wetting transitions in the presence of an external field as well as other related problems.<sup>18</sup> Let us approach this topic by asking for the effective force between a rigid, absorbing wall and a nearby random walk as illustrated in Fig. 14.

We learn from (5.5) that the partial partition function for a walk which starts at a small distance,  $a$ , from a wall at the origin and, after  $n$  steps, reaches the point  $x$  is given by

$$Q_n^W(x) \sim ae^{-\alpha n} x e^{-x^2/2nb^2} / n^{3/2} \tag{9.1}$$

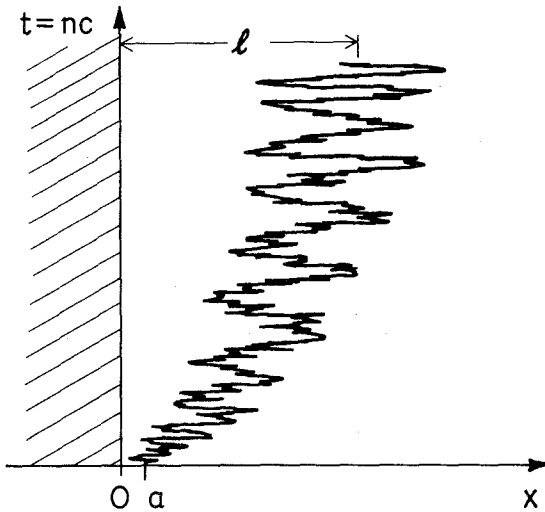


Fig. 14. Portrayal of a walk near an adsorbing wall showing the drift of the most probable position of the walker,  $l = bn^{1/2}$ , away from the wall under the influence of the effective wall-walk force of repulsion.

<sup>17</sup> The interface width  $b$  should be comparable to the transverse correlation length,  $\xi_{\perp}$ , in the bulk phases.  
<sup>18</sup> Attention may be drawn to Natterman's further developments of interface phenomenology to include dipolar couplings, random field effects, etc.<sup>(44)</sup>

The most probable distance from the wall after  $n$  steps is thus

$$l = bn^{\frac{1}{2}} \quad (9.2)$$

The mean distance, of course, varies similarly with  $n$ . The total partition function for  $n$  step-walks near the wall is

$$Z_n^W = \int dx Q_n^W(x) \sim e^{-\sigma n} / n^{\frac{1}{2}} \quad (9.3)$$

and so the reduced free energy per step at the  $n$ th step is given by

$$f_n = -\ln(Z_{n+1}/Z_n) = \sigma + \frac{1}{2} \ln(1 + n^{-1}) \quad (9.4)$$

Now re-express this result in terms of  $l$  and expand for  $l^2/b^2 > 1$ . This tells us that the free energy per step [i.e., per unit of length,  $c$ , of walk parallel to the wall in the  $(x, y)$  plane] varies with  $l$ , the (most probable or mean) distance from the wall, as

$$f(l) = \sigma + \frac{1}{2} \frac{b^2}{l^2} + O\left(\frac{b^4}{l^4}\right) \quad (9.5)$$

The first term,  $\sigma$ , represents simply the reduced free energy per step of a free walk which, naturally, is realized when  $l \rightarrow \infty$ . The further terms are thus due to the interactions between the walk and the wall; indeed they correspond to an *effective force* with a repulsive, i.e., positive *potential*

$$W(l) \approx \frac{1}{2} k_B T \frac{b^2}{l^2} \quad (l/b \gg 1) \quad (9.6)$$

per step [or per length of walk  $c$  in the  $(x, t)$  plane]. The dependence of this potential on temperature serves as a reminder that the origin of the force lies in the *loss of entropy* a walk incurs when the walker approaches but cannot penetrate the absorbing wall.

How literally can we accept the result (9.6)? Does it apply in other circumstances? To test the interpretation, consider a walk which is confined between *two* absorbing walls at spacing  $2L$ : see Fig. 15 which, in part (b), also shows the total effective potential, or free energy increment due to the walls,

$$\Phi(l; L) = W(l) + W(2L - l) \quad (9.7)$$

constructed by supposing that each wall may be regarded as acting independently on the walker. By symmetry, the most probable position of the walker is at  $l_0 = L$ ; but this location can, alternatively, be regarded as that which minimizes  $\Phi(l)$ . Thus we anticipate that the appropriate walk free energy can be written in the form

$$f_2(L) \approx \sigma + 2c_2 \frac{1}{2} (b^2/L^2), \quad \text{for} \quad L^2/b^2 \gg 1 \quad (9.8)$$

If (9.6) is taken literally the coefficient here has the value  $c_2 = 1$ .

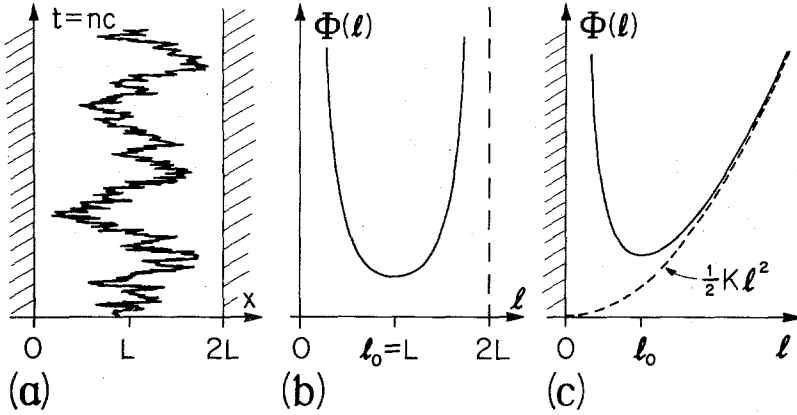


Fig. 15. (a) Depiction of a random walk between two absorbing walls at  $x = 0$  and  $x = 2L$ ; (b) the total effective walk-wall potential,  $\Phi(l)$ , for a walk between two walls; (c) the effective potential for a walk in a harmonic well with an absorbing wall at  $x = 0$ .

On the other hand, let us return to the original lattice model of the walk described in Section 1. It is easy to see that the partial partition functions satisfy the *difference equation*

$$Q_{n+1}(x) = w_{-1} Q_n(x + a) + w_0 Q_n(x) + w_1 Q_n(x - a) \quad (9.9)$$

Two absorbing walls at  $x = \pm L$  are then described by the boundary conditions

$$Q_n(L) = Q_n(-L) = 0 \quad (\text{all } n) \quad (9.10)$$

A linear difference equation with constant coefficients is easily solved: the form (9.8) turns out to be quite correct but one discovers that the coefficient has the exact value<sup>(43)</sup>

$$c_2 = \pi^2/8 \simeq 1.2337 \quad (9.11)$$

The description in terms of two superposable wall forces is thus qualitatively exact; quantitatively it is in error only by about 19%! Incidentally, the value of  $c_2$  remains unchanged if the walk is allowed to make *arbitrarily large* weighted jumps at each step (provided only that  $b^2$  remains finite).<sup>(43)</sup>

Further, more challenging tests are possible. Suppose that the walker moves in an external potential described by

$$U(x) = V(x)/k_B T \quad (9.12)$$

so that a Boltzmann factor  $e^{-U(x)}$  is to be associated with each step on which a walker arrives at or remains on the site  $x$ . The recursion relation (9.9) thus becomes

$$Q_{n+1}(x) = e^{-U(x)} [w_{-1} Q_n(x + a) + w_0 Q_n(x) + w_1 Q_n(x - a)] \quad (9.13)$$

This equation (which is well known in studies of the solid-on-solid model of an interface in an external field<sup>(15-18)</sup>) is, in general, hard to solve exactly. However, if  $U(x)$  varies smoothly, one may go to the continuum limit in  $x$  and  $t$  and obtain the *Schrödinger-like diffusion equation*

$$\frac{\partial Q}{\partial t} = \frac{1}{2}b^2 \frac{\partial^2 Q}{\partial x^2} - [\sigma + U(x)] Q \quad (9.14)$$

for the continuum partial partition function,  $Q(x; t)$ . [In taking the limit the weights  $w_i$  must be written in appropriate form and the free energies  $f$  and  $\sigma$ , and the potential,  $U(x)$ , must be redefined to refer to unit time: then the Boltzmann factor in (9.13) becomes  $e^{-cU(x)}$  with  $c \rightarrow 0$ , and so on.] This generalized diffusion equation is somewhat more tractable than the discrete equation as we shall see.

As a second test problem consider a walker moving in a harmonic potential well,

$$U(x) = \frac{1}{2}Kx^2 \quad (9.15)$$

which acts outside an absorbing wall at the origin; see Fig. 15c. If  $K$  is not too large  $U(x)$  varies slowly on the scale of  $b$  and, heuristically, we can write down the total free energy for a walk at distance  $l$  from the wall

$$f_3(K; l) = \sigma + \Phi(l) \approx \sigma + \frac{b^2}{2l^2} + \frac{1}{2}Kl^2 \quad (9.16)$$

Minimization yields the most probable walk location as

$$l_0 = b^{1/2} / K^{1/4} \quad (9.17)$$

and substitution in (9.16) then shows that the free energy should vary with  $K$  as

$$f_3(K) = \sigma + c_3 b \sqrt{K} \quad (9.18)$$

with  $c_3 = 1$ .

To check this we must solve the diffusion equation (9.14) subject to the boundary condition  $Q(0; t) = 0$  (all  $t$ ). Since, as one learns in elementary quantum mechanics, harmonic potentials go well with Schrödinger's equation, one can actually find an exact solution for all  $t$  with the general initial condition  $Q(x, 0) = \delta(x - x_0)$ . However, since only the asymptotic free energy is required, it is easiest to ask merely for the long time behavior and hence to solve the corresponding ground-state Schrödinger eigenvalue problem. In this particular case, however, it is simplest just to guess a trial solution of the form

$$Q(x, t) = e^{-ft} x e^{-x^2/2l_0^2} \quad (9.19)$$

One readily checks that this solves (9.14) only if  $l_0$  is given by (9.17). Thus the most probable walk location is given *exactly* by the heuristic arguments! From (9.19), (9.17), and (9.14) one discovers that the form (9.18) for the free energy is, again, quite correct. This time, however, the coefficient  $c_3$  is in error by about 33%, the exact value being  $c_3 = 3/2$ ; but this reduced accuracy is not really surprising since the direct effects of the harmonic potential on the walker were ignored in writing (9.16). Clearly a walker is restricted even by a pure harmonic potential and so loses some entropy: the effect corresponds precisely to the zero-point motion in a pure harmonic well which yields a free energy increment

$$\Delta f_0 = \frac{1}{2} b \sqrt{K} \equiv \frac{1}{2} b \left[ (d^2 U / dx^2) \right]^{\frac{1}{2}} \quad (9.20)$$

(corresponding to the usual zero point energy  $\frac{1}{2} h\nu$ ). If this is added to (9.18) with  $c_3 = 1$  the exact answer is recaptured! The second form written here for  $\Delta f_0$  suggests that the heuristic ansatz leading to (9.7) and (9.16) could be improved for slowly varying potentials,  $U(x)$ , by adding a local term,  $\Delta f_0(l)$ , evaluated from the second derivative in accord with (9.20).

The tests presented above should convince one that the effective wall-walk potential,  $W(l)$ , found in (9.6) will give a good general account of the effects of walls and other external potentials on an otherwise random walker. What about interactions between two or more walks? Consider two dissimilar walkers at separation  $l$ : from the viewpoint of the first walker the second may be approximated by a wall at distance  $l$ , and vice-versa for the second walker. Thus we would guess that the total entropy loss should be described by the *walk-walk interaction potential*

$$W(l) \approx k_B T \frac{b_1^2 + b_2^2}{2l^2} \quad (9.21)$$

Certainly, this reduces correctly to (9.6) when either  $b_1$  or  $b_2$  vanish, a nondiffusing walk corresponding, as before, to a stationary wall. More generally, however, one can check the validity of (9.21) by recalling the result (4.18) for two dissimilar vicious walkers and repeating the general reasoning that led to (9.6).

A more stringent test is provided by considering  $p = 3$  similar vicious walkers for which the total free energy follows from (4.2) or (4.9) [the coefficient  $\frac{1}{2}$  in (9.4) being replaced, in general, by  $\frac{1}{4}p(p-1)$ ]. By symmetry, the three walkers will on average be equally spaced and from (4.7) and (4.8) one finds that the most probably spacing is  $l = \sqrt{(3/2)bn^{\frac{1}{2}}}$ . If this is used in (9.21) to evaluate the sum  $2W(l) + W(2l)$ , which allows for *all* pairs of walk interactions, the exact result for the free energy is again reproduced.

Since the expression (9.21) for the effective forces felt by a walk passes its trials with flying colors, let us try it in some applications.

## 10. CRITICAL PREWETTING

Consider the phase diagram of a fluid system, as sketched in Fig. 16, which exhibits a first-order transition from phase *A*, say, “vapor,” to phase *B*, say, “liquid” on a phase boundary  $\mu = \mu_\sigma(T)$ .<sup>(45,46)</sup> It is convenient to define the external bulk field by

$$h = \mu - \mu_\sigma(T) \quad (10.1)$$

Then our previous discussion of the two-dimensional wetting transition of a wall attractive to phase *B* but in contact with bulk phase *A* was confined to the phase boundary itself, i.e.,  $h = 0$ . Somewhat more precisely, we required  $h = 0^-$  — since an infinitesimal negative field was needed to ensure the presence of bulk *A* phase, as illustrated in Fig. 8. When  $T$  increased a critical wetting transition was reached at  $T = T_{cW}$ ; this is indicated by the open circle in Fig. 16. For  $T \geq T_{cW}$  a wetting layer of macroscopic thickness,  $l_W = \infty$ , covers the wall; the dots along the phase boundary in Fig. 16 denote this wet state.

Now a wetting film of *finite* thickness,  $l_W$ , will persist even in the presence of a negative field,  $h = -|h|$ . The wetting transition can then be described by saying that  $l_W(T, h)$  *remains finite* as  $h \rightarrow 0^-$  — for  $T < T_{cW}$  but *diverges to infinity* when  $h \rightarrow 0^-$  — if  $T \geq T_{cW}$ . But what is the form of this divergence of  $l_W(T, h)$  as  $h$  vanishes? And, how do the thickness  $l_W(T, h)$ ,

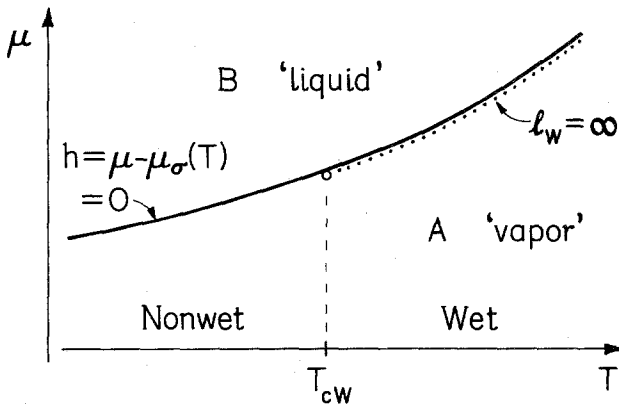


Fig. 16. Bulk phase diagram showing a critical wetting transition at  $T = T_{cW}$ . (See also Refs. 45 and 46.)

and the wall free energy,  $f(T, h)$ , vary with  $T$  at nonzero  $h$  near the wetting transition? These questions have been discussed by Abraham and Smith<sup>(47)</sup> on the basis of the Schrödinger-like diffusion equation (9.14). Here we present a heuristic treatment which yields an understanding of their results and goes slightly further in some respects.

Consider, first, the wetting film in a field  $h = -|h|$  well above the transition at  $T_{cW}$ . Adopting the previous picture (see Fig. 8) we construct the free energy for a film of thickness  $l$  as

$$f(T, h; l) = \sigma - h_1 + |h| \frac{cl}{\bar{a}^2} + \frac{1}{2} \frac{b^2}{l^2} \quad (10.2)$$

The first term on the right is the (reduced) tension of the free interface; the second represents the net short range attraction of the wall for phase  $B$ ; in the third term  $cl$  represents the area of the interface per step (parallel to the  $y$  axis), while one has

$$\bar{a}^2 = k_B T / \Delta\rho \quad (10.3)$$

in which  $\Delta\rho$  is the jump in density across the bulk phase boundary. (Recall that  $\mu$  couples to the density,  $\rho$ .) Finally, the last term in (10.2) represents the interface-wall interaction in accord with (9.6). Minimization on  $l$  yields a (most probable) wetting layer thickness diverging as

$$l_W \approx \bar{b} / |h|^{1/3}, \quad \text{with} \quad \bar{b} = (b^2 \bar{a}^2 / c)^{1/3} \quad (10.4)$$

that is with an exponent  $\nu_W = 1/3$ . The free energy then varies for small fields as

$$f(T, h) \approx \sigma - h_1 + \frac{3}{2} B |h|^{2/3} \quad (10.5)$$

with  $B = (bc / \bar{a}^2)^{2/3}$ . As in the tests of the wall-walk force law we should anticipate that the factor  $3/2$  is not exact although it should be accurate to 20% or so.

Now to discuss the transition region we must allow for the situation, illustrated in Fig. 8, in which, statistically, the wetting film is composed of a distribution of droplets of  $B$ -like phase adhering to the wall. The crucial new feature that arises is the need to include the external field,  $h$ , in the bubble generating function; thus the partition function  $Q_n^B$ , for a bubble of length  $n$  (in units of  $c$ ), should have a factor

$$\exp \left[ -n(\sigma - h_1) - \bar{A}_n |h| / \bar{a}^2 \right] \quad (10.6)$$

where  $\bar{A}_n$  is the mean area of a bubble. If the external field can be neglected, the area is given by (7.7) which can be written

$$\bar{A}_n = \tilde{a}^2 n^{3/2} \quad \text{with} \quad \tilde{a}^2 = (\pi / 4\sqrt{2}) bc \quad (10.7)$$

One is therefore tempted merely to insert a factor  $\exp(-k_0|h|n^{3/2})$  with

$$k_0 = \tilde{a}^2/\bar{a}^2 \tag{10.8}$$

[in accord with (10.2)] into the original form (6.10) for  $Q_n^B$ . To do this, however, would overlook the effects of the field itself on the shape and size of a typical bubble.

In order to account for the field properly one should solve the recursion relation (9.13) or the Schrödinger diffusion equation (9.14) with a linear potential  $U(x) \propto |h|x$ . In the latter case, closed-form but complex results could be anticipated in terms of Airy functions.<sup>(47)</sup> However, we can embody the physically important features in a simple approximation which can be explained with the aid of Fig. 17. For a sufficiently small droplet the field has negligible effect on the shape and we may use (10.7) in (10.6) to obtain a satisfactory representation of  $Q_n^B$ . But once the maximum width for a typical free bubble, namely,  $x_n \approx b(\frac{1}{2}n)^{\frac{1}{2}}$  [see (7.6)] exceeds the wetting film thickness for the field in question, namely,  $l_w(h) \approx \bar{b}/|h|^{1/3}$  [see (10.4)], the width of a bubble will be effectively limited by the field. Equating  $x_n$  to  $l_w$  shows that this crossover in bubble shape occurs at

$$n_0(h) \approx 2(\bar{b}/b)^2|h|^{-2/3} \tag{10.9}$$

For  $n > n_0$  the bubble area will, except for end effects decreasing as  $(n_0/n)$ , be given simply by  $\bar{A}_n = ncl_w$  so that  $\bar{A}_n|h| \sim n|h|^{2/3}$  which correctly reflects the result (10.5). Thus the simplest approximation for  $Q_n^B$  is constructed by using this form in (10.6) for  $n \geq n_0(h)$  but to use (10.7) for  $n \leq n_0(h)$ . A better approach is to utilize a smooth changeover function chosen to preserve the analyticity at small  $h$  which the exact generating function must enjoy. A simple but satisfactory option is to replace  $n$  in  $(\bar{A}_n/n)$  and in the

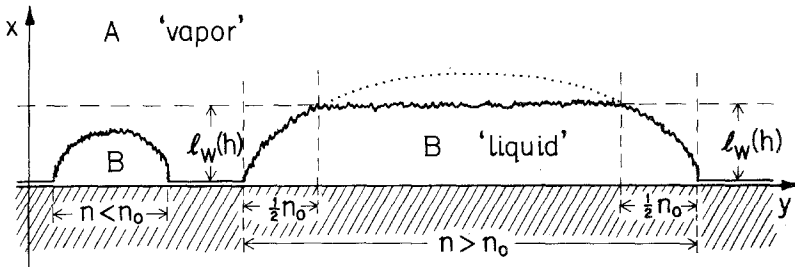


Fig. 17. Droplets or bubbles of "liquid," B, adhering to a wall in the presence of an external field,  $h$ , which favors the bulk "vapor" phase, A. Droplets of length less than  $n_0(h)$  (in units of  $c$ ) are effectively uninfluenced by  $h$  but when  $n$  exceeds  $n_0$  the width of a droplet is limited by  $l_w(h)$ .

prefactor for  $Q_n^B$  by  $\tilde{n}(h) \equiv n/(1 + k_1^3 n^3 h^2)^{1/3}$  which becomes proportional to  $n_0(h)$  when  $n \rightarrow \infty$ . This yields the physically reasonable approximation

$$Q_n^B z^n \approx q_0 \frac{e^{-n\Delta f}}{n^{3/2}} (1 + k_1^3 n^3 h^2)^{\frac{1}{2}} \exp \left[ \frac{-k_0 n^{3/2} |h|}{(1 + k_1^3 n^3 h^2)^{1/6}} \right] \tag{10.10}$$

in which

$$\Delta f = \sigma - h_1 - f \tag{10.11}$$

The changeover parameter,  $k_1$ , should now be chosen so that

$$k_0/k_1^{\frac{1}{2}} \equiv \tilde{\alpha}^2/\tilde{\alpha}^2 k_1^{\frac{1}{2}} = \frac{3}{2} B \equiv \frac{3}{2} (bc/\tilde{\alpha}^2)^{2/3} \tag{10.12}$$

This serves to ensure that (10.5) is reproduced well above the transition. Other limits are readily checked.

Whichever approximation is adopted, it is not hard to see that, near its singularity, the bubble generating function approaches the scaling behavior

$$G_B(z, h) - G_c \approx -|h|^{\frac{1}{3}} \Gamma \left( \frac{\Delta f}{|h|^{\frac{2}{3}}} \right) \tag{10.13}$$

Indeed this must also be a consequence of the exact analysis. The approximation (10.10) yields the closed expression

$$\Gamma(s) = q_0 k_1^{\frac{1}{2}} \int_0^\infty \frac{dr}{r^{3/2}} \left\{ 1 - (1 + r^3)^{\frac{1}{2}} \exp \left[ -sr/k_1 - k_2 r^{3/2}/(1 + r^3)^{1/6} \right] \right\} \tag{10.14}$$

where  $k_2 = k_0/k_1^{3/2}$ ; although not exact, this reproduces the correct results in the various limits and should be useful for practical purposes. From (10.13) the scaling behavior of the wall free energy follows straightforwardly by the methods of Section 6. One obtains

$$f \equiv \frac{\Sigma_W(T, h)}{k_B T} \approx \sigma - h_1 - |h|^{\frac{2}{3}} \Upsilon \left( \frac{T - T_{cW}}{|h|^{\frac{1}{3}}} \right) \tag{10.15}$$

which, again, is necessarily a consequence of the more exact theory. In particular, the exponents entering are exact.<sup>(47)</sup> The scaling function  $\Upsilon(u)$  can be expressed in terms of  $\Gamma(s)$ . If one accepts the approximation (10.14) as adequate, or considers the possible behavior of  $G_B(z; h)$  more generally, one discovers that there is *no transition* in the presence of a nonzero field.<sup>(47)</sup> Thus the phase diagram in Fig. 16 correctly represents the situation.

The general nature of the scaling function  $\Upsilon(u)$  follows from the known limiting behavior. Thus,  $\Upsilon(u)$  approaches  $-\frac{3}{2} B$  as  $u \rightarrow +\infty$  so reproducing (10.5). On the other hand when  $|h| \rightarrow 0$  at fixed  $T < T_{cW}$  so

that  $u \rightarrow -\infty$  the scaling function behaves as  $A_0 u^2$  which yields the original critical wetting expression (7.4). One may hope that it will eventually prove possible to check these predictions for two-dimensional wetting in the laboratory.

## 11. ISING MODEL CORRELATIONS IN TWO DIMENSIONS: ANOMALOUS DECAY LAW

Consider a two-dimensional Ising model on, say, a rectangular lattice with a spin variable  $s_{xy} = \pm 1$  at each lattice site  $(x, y)$ . In accord with our previous conventions we will take the  $x$  and  $y$  lattice spacings as  $a_{\perp} \equiv a$  and  $a_{\parallel} \equiv c$ , respectively. The net, two-point correlation function is defined, in the standard way, by

$$C(x, y) = \langle s_{00} s_{xy} \rangle - \langle s_{00} \rangle \langle s_{xy} \rangle \quad (11.1)$$

The decay of the correlations with distance is a matter of perennial interest! Away from the immediate critical region the Ornstein-Zernike theory should apply to the two-point function; this predicts

$$C(x, y) \approx D_{\theta} e^{-\kappa_{\theta} r} / r^{\frac{1}{2}}, \quad \text{as } r \rightarrow \infty, \quad \text{for } d = 2 \quad (11.2)$$

where  $\kappa_{\theta} \equiv 1/\xi(T, \theta)$  denotes the inverse correlation length for the direction  $\theta$ , measured, say, from the  $y$  axis, while  $r$  is the radial distance. Of course,  $\kappa_{\theta}$ , and the amplitude,  $D_{\theta}$ , depend on the temperature and the (reduced) magnetic field,  $h$ ; the exponent  $\frac{1}{2}$  of the power in the decay law is, however, universal (away from criticality)<sup>(48)</sup>; in fact, it reflects a dominant simple pole at  $k = \pm i\kappa_{\theta}$  in the Fourier transformed correlation function,  $\hat{C}(\vec{k})$ .

The Ornstein-Zernike prediction (11.2) is verified by the exact calculations of the two-point correlations for planar Ising models in zero field ( $h = 0$ ) above  $T_c$ .<sup>(49-52)</sup> Perturbation expansions allowing for the field  $h$  suggest that (11.2) remains valid in the presence of a nonzero field.<sup>(48,53,54)</sup> However, the exact calculations for zero field below  $T_c$  show that (11.2) is violated<sup>(49,52)</sup>; instead, the two-point correlation function<sup>19</sup> obeys the *anomalous decay law*

$$C(x, y) \approx D_{\theta} e^{-\kappa_{\theta} r} / r^2 \quad (d = 2, h = 0, T < T_c) \quad (11.3)$$

that is, the exponent  $\frac{1}{2}$  becomes 2. This corresponds to a branch point and

<sup>19</sup> Strictly, one must take the limit  $h \rightarrow 0 \pm$  or replace the product  $\langle s_{00} \rangle \langle s_{xy} \rangle$  by the square of the spontaneous magnetization,  $m_0(T)$ , or by the long range order,  $\langle s_{00} s_{\infty \infty} \rangle$ .

associated cut in the complex  $k$  plane in place of the Ornstein–Zernike pole.

The analysis leading to the exact solutions throws little light on the reason for this anomalous decay; nor does it indicate whether or not it should persist in the presence of a small field below  $T_c$ . This issue has been addressed in a general context using the *transfer matrix approach*<sup>(48,54)</sup> and it has been shown<sup>(55)</sup> that the anomalous behavior below  $T_c$  is, in fact, special *both* to  $d = 2$  dimensions *and* to zero field. To check this conclusion, McCoy and Wu<sup>(56)</sup> have tackled the problem of including a small field in the exact calculations for the two-dimensional Ising model; they discovered the mathematical mechanism by which the behavior (11.3) goes over to (11.2) as the field  $h$  is switched on<sup>20</sup> but, again, rather little physical insight can be gleaned! More recently, Abraham<sup>(57)</sup> has treated the problem approximately and shown how the exact results can be understood heuristically on the basis of a bubble picture. As we will show, simplifying Abraham's analysis still further, the issue becomes isomorphic to the behavior of a wetting layer in the presence of a bulk field: essentially, then, we will merely recast the arguments of the previous section in a new language!

The starting point is explained in Fig. 18. Low-temperature expansions for Ising models are constructed by turning over spins from the fully aligned or  $+$  state ( $s_{xy} = +1$  all  $x, y$ ). One thus discovers that contributions to the two-point correlation function,  $C(x, y)$ , arise only from configurations in which both sites  $(0, 0)$  and  $(x, y)$  are *linked* by a chain of neighboring overturned spins so that they reside in the same island of  $-$  spins. The energy of such a configuration in *zero field* is determined solely by the total length of *perimeter* of the islands of  $-$  spins: in the presence of a field there is an additional contribution proportional to  $h$  and to the total *area* of the islands. At *large separations*,  $r \gg a, c$ , the dominant contributions will thus come from those islands which just reach from  $(0, 0)$  to  $(x, y)$ ; however, there is entropy to be gained if the perimeters of the islands are allowed to wander. In *zero field*, therefore, we anticipate that the

<sup>20</sup> The McCoy–Wu analysis<sup>(56)</sup> is based on a formal expansion in powers of the field,  $h$ . In the complex  $k$  plane the anomalous branch cut present in zero field breaks up into a sequence of poles. McCoy and Wu calculate the locations and residues of the poles near the tip of the cut for small  $h$ . The location of these poles is also discussed from a perspective somewhat closer to that developed here (and in Ref. 55) by Stone.<sup>(37)</sup> However, as pointed out by Abraham<sup>(57)</sup> the approximate real-space expression presented for  $C(x, y)$  by McCoy and Wu is actually inadequate for large  $(x, y)$  as can be seen by calculating the fluctuation sum, which should yield a finite value for the susceptibility,  $\chi(T, h)$ , but which, in fact, diverges. Discussions with Barry M. McCoy on these issues are appreciated.

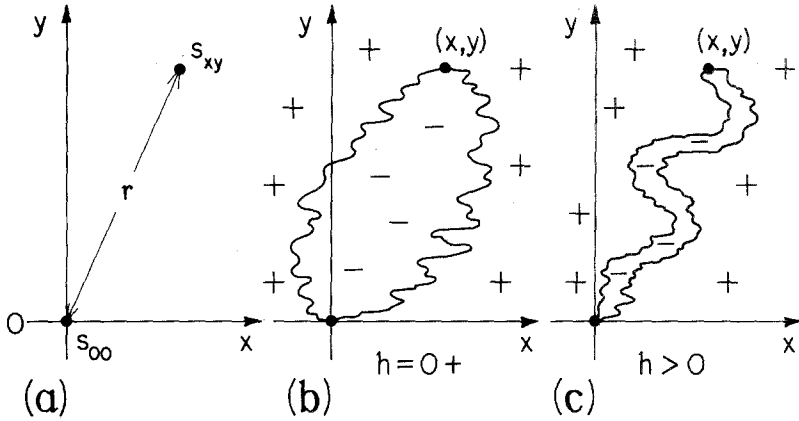


Fig. 18. Configurational interpretation of the net spin-spin correlation function,  $C(x, y)$ , of a two-dimensional Ising model below  $T_c$  [see (11.1)], (b) in the case of zero field (in the “up” or “+” phase) and (c) in a small positive field showing the narrowing of a typical subdomain of overturned spins which contributes to the dominant behavior of  $C(x, y)$  for large  $r$ .

behavior will be determined by a “bubble” of  $-$  spins which constitute a small subdomain as illustrated in Fig. 18b. The free energy to be associated with the perimeter is thus just the interfacial tension,  $\Sigma(T)$ , times the total length.

Let us now suppose that the angle  $\theta$  is relatively small ( $\theta^2 \approx x^2/y^2 \ll 1$ ): then, as previously, we may regard the two sides of the subdomain or bubble stretching from  $(0, 0)$  to  $(x, y)$ , as *two strings* representing the paths of two vicious random walkers on the  $(x, y)$  plane with  $y \equiv t = nc$  denoting time. The statistical weight of the subdomain is then proportional to the partial walk partition function and, in turn, yields the correlation function in leading order. From the expression (4.12) for the reunion of vicious walkers we thus obtain

$$C(x, y) \propto e^{-2\sigma n - \frac{1}{2}(2x^2/b^2n)} / n^2 \tag{11.4}$$

the crucial exponent coming merely from  $\frac{1}{2}p^2$  at  $p = 2$ . The free energy per step,  $\sigma$ , required here is that for an interface running parallel to the  $y$  axis so that  $\sigma = c\Sigma_{\parallel}/k_B T$ . Now it is not hard to show that the diffusivity of a walker representing an interface should be related to the interfacial tension via<sup>(43)</sup>

$$b^2 \approx ck_B T / \tilde{\Sigma}(T) \quad \text{with} \quad \tilde{\Sigma} = \Sigma_0 + \Sigma'' \tag{11.5}$$

Here we have used the fact that the interface is rough so that  $\Sigma(T; \theta)$  is a

differentiable function of the angle  $\theta$ ; then one has<sup>(43)</sup>

$$\Sigma_0 = \Sigma(T; 0) \equiv \Sigma_{\parallel} \quad \text{and} \quad \Sigma'' = \left( \frac{\partial^2 \Sigma}{\partial \theta^2} \right)_{\theta=0} \quad (11.6)$$

Finally a little algebra shows that (11.4) can be rewritten, up to errors of order  $\theta^4 \approx x^4/y^4$  in the exponent, as

$$C(x, y) \propto e^{-2\Sigma(T; \theta)r/k_B T} / r^2 \quad (11.7)$$

where  $r^2 = x^2 + y^2$ . This agrees with the exact anomalous decay law (11.3) and implies a definite relation between the inverse *correlation length* and the *surface tension* at angle  $\theta$ , namely,

$$1/\xi(T; \theta) \equiv \kappa_\theta = 2\Sigma(T; \theta)/k_B T \quad (11.8)$$

But this relation is, in fact, an *exact* result for the two-dimensional Ising model for all  $T < T_c$ !<sup>(52,58,59)</sup> It is also exact for the ordered regions of Baxter's hard square/hexagon model for directions parallel to the square lattice axes.<sup>(36)</sup> Thus the bubble "picture" for the large distance behavior of the correlations in zero field has proved surprisingly accurate. Notice that the factor 2 in (11.8) corresponds to the *two* strings defining the perimeter of the dominant bubble, while the anomalous power  $1/r^2$  arises directly from the diffusive repulsion between the two strings.

What will happen in a nonzero magnetic field? As explained, the statistical weight of a bubble will be reduced by a factor representing the action of the field on the *area* of the bubble. This is precisely the same effect as in the wall wetting analyzed in the previous section. For  $\theta$  not too large and  $y$  less than  $cn_0(h)$ , where  $n_0 \sim |h|^{-2/3}$  may be taken from (10.9), the field will have negligible effect on  $C(x, y)$ . For larger values of  $r$ , however, the width of the bubble will saturate at  $\Delta x \approx b(\frac{1}{2}n_0)^{1/2} \sim |h|^{-1/3}$  and, instead of two freely diffusing strings, we will be left with a *single* double string.<sup>(57)</sup> As suggested in Fig. 18c, this double string will diffuse but it is unrestricted by collisions. Thus we can put  $p = 1$  in the general walker expressions and obtain

$$C(x, y) \propto e^{-\sigma_2 n - \frac{1}{2}x^2/b^2 n} / n^{\frac{1}{2}} \quad (11.9)$$

Thus the original  $1/r^{\frac{1}{2}}$  decay law is restored by the field, as anticipated. The walk tension,  $\sigma_2$ , now denotes the free energy per step of a double walk. But this must depend on the magnetic field in the same way as the surface free energy in the wall wetting problem. From (10.5) we can thus read off the dependence of the correlation length on the field as

$$c/\xi_{\parallel}(T, h) - c/\xi_{\parallel}(T, 0) \approx B|h|^{2/3} \quad (11.10)$$

This singular variation with  $h$  is confirmed by the exact calculations and by

the approximate but more detailed analyses.<sup>(56,57)</sup> The diffusivity  $b_2^2$  appearing in (11.9) must reduce to  $\frac{1}{2}b^2$  as  $h \rightarrow 0$  but may have a nontrivial field dependence which should also be reflected in the angular dependence of  $\xi(T, h; \theta)$ .

An approximate crossover form for the correlation function may be constructed along the lines used in writing down (10.10). The essential, and exact feature is a scaling behavior in terms of the combination  $r|h|^{2/3}$ ; this leads to a prefactor  $|h|$  in the long-range behavior in a field in agreement with the exact results.<sup>(56)</sup> Although an approximate formula analogous to (10.10) will probably be fairly accurate, its Fourier transform will not exhibit the correct mathematical structure for  $h \neq 0$ . In fact, the exact analysis of Wu and McCoy<sup>(56)</sup> shows that the anomalous cut in the  $k$  plane breaks up into a sequence of simple poles at spacing of order  $|h|^{2/3}$ . However, Abraham's more detailed discussion of the bubble approximation on the basis of the Schrödinger-like diffusion equation,<sup>(57)</sup> does reproduce this feature correctly. The essence of the matter is thus once more captured by the heuristic walk/interface/string picture.

## 12. COMMENSURATE-INCOMMENSURATE TRANSITIONS

Under variation of temperature and chemical potential (or pressure, etc.) a commensurate phase may undergo a transition into an *incommensurate*

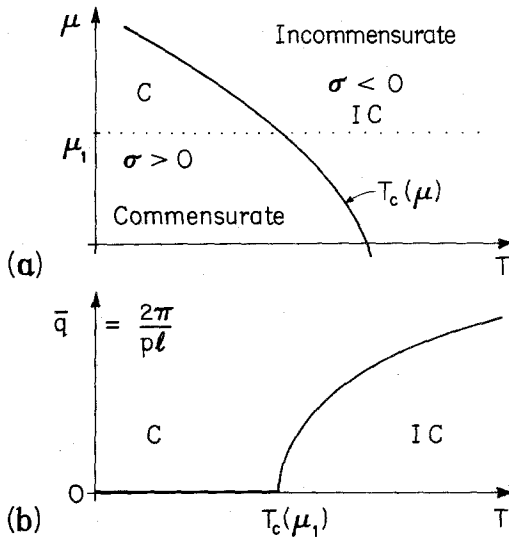


Fig. 19. (a) Phase diagram showing a commensurate-incommensurate (or C-IC) transition in the  $(T, \mu)$  plane; (b) variation of the incommensurability,  $\bar{q}(T, \mu)$  on the locus  $\mu = \mu_1$ .

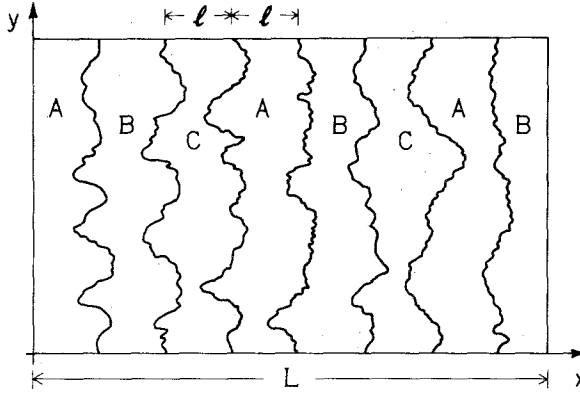


Fig. 20. Schematic representations of a  $3 \times 1$  incommensurate phase showing domain walls at mean spacing  $l$ .

rate phase; a typical phase diagram is sketched in Fig. 19a. Now, from the work of many authors<sup>21</sup> we know that a uniaxial incommensurate phase can, not too far from the transition, be viewed as a sequence of domains of commensurate phase separated by parallel sheets of domain walls or interfaces at some mean spacing  $l$ . This characterization of an incommensurate phase derived from a two-dimensional  $p \times 1$  commensurate phase is illustrated in Fig. 20. If there are  $N$  walls, say, parallel to the  $y$  axis, in a length  $L$  along the  $x$  axis the linear density of walls,  $N/L = 1/l$ , may be regarded as a type of order parameter for the incommensurate phase; in practice one usually defines the *incommensurability*

$$\bar{q}(T, \mu) \equiv 2\pi/pl \tag{12.1}$$

which can be observed in scattering experiments as the displacement of an adsorbate Bragg peak from the associated commensurate Bragg peak (or reciprocal lattice vector) of the underlying substrate lattice. If

$$t \propto T - T_c(\mu) \tag{12.2}$$

measures the distance from the commensurate-incommensurate (C-IC) phase boundary,  $T_c(\mu)$ , one may expect a power law variation

$$\bar{q} \approx Q_0 t^{\bar{\beta}} \quad (t \rightarrow 0+) \tag{12.3}$$

where the value of the exponent  $\bar{\beta}$  is of prime interest (see Fig. 19b).

This problem has been approached by a variety of fairly sophisticated mathematical techniques,<sup>(40,60-63)</sup> in particular by representing the walls as

<sup>21</sup> See the review by Bak<sup>(60)</sup> and references therein.

one-dimensional *fermions* moving on the  $x$  axis with, just as in the interpretation in terms of walkers, the  $y$  axis representing time.<sup>22</sup> But, as pointed out by Pokrovsky and Talapov,<sup>(40)</sup> who were the first to calculate the value of  $\bar{\beta}$ , the correct answer is readily obtained and understood by thinking about the *interactions* between the domain walls.<sup>(43)</sup> If  $W(l)$  denotes the interaction potential of one domain wall with a neighbor at mean separation  $l$ , the singular part of the free energy density can be constructed as

$$f_s(T, \mu; l) \approx L^{-1} [N\sigma + NW(l)/k_B T] \quad (12.4)$$

where  $\sigma = \sigma(T, \mu)$  is the interfacial tension of an isolated domain wall parallel to the  $y$  axis. Now, in the commensurate phase the tension  $\sigma$  is positive and an isolated wall is stable. However, as the C-IC transition is approached  $\sigma$  vanishes and becomes negative in the commensurate phase: the resulting instability leads to the appearance of many walls. To leading order we may thus write

$$\sigma \approx -\sigma_1 t \quad \text{with} \quad \sigma_1 > 0 \quad (12.5)$$

But, as we have seen in Section 9, we should anticipate repulsive forces acting between walls which will stabilize the incommensurate phase as an array of walls. At large separations,  $l$ , which are relevant near the transition, we may use the basic result (9.21) for the interface interactions and thus conclude<sup>(40,43)</sup>

$$f_s(T, \mu; l) \approx -\sigma_1/tl + b_0^2/l^3 \quad (12.6)$$

where the modified wall diffusivity,  $b_0^2 \propto b^2$ , allows for the additional interactions between further neighboring walls. Note that the value of the isolated wall diffusivity,  $b^2$ , is given in terms of the interfacial tension as in (11.5).<sup>(43)</sup>

Minimizing on  $l$ , as previously, yields the mean value

$$1/l = (\sigma_1/3b_0^2)^{1/2} t^{1/2} \quad \text{for} \quad t \geq 0 \quad (12.7)$$

whence, in agreement with the more sophisticated theories,<sup>(40)</sup> we conclude  $\bar{\beta} = \frac{1}{2}$  (for  $d = 2$ ).<sup>23</sup> Likewise the free energy is given by<sup>(2)</sup>

$$\begin{aligned} f_s(T, \mu) &= 0, & \text{for} & \quad T \leq T_c(\mu) \\ &\approx -A_0 t^{3/2}, & \text{for} & \quad T \geq T_c(\mu) \end{aligned} \quad (12.8)$$

where  $A_0 = 2(\sigma_1^3/3b_0^2)^{1/2}$ . Thus the transition is critical but the exponents are *nonclassical*: in fact the specific heat diverges when  $T$  approaches  $T_c(\mu)$

<sup>22</sup> As mentioned in Section 5, an interesting early paper using fermions to represent strings or interacting walkers is by de Gennes.<sup>(4)</sup>

<sup>23</sup> The generalization of this result to other values of  $d$  is considered in Refs. 43 and 44.

from above as  $t^{-\alpha}$  with exponent

$$\alpha = \frac{1}{2} \tag{12.9}$$

However, there is *no divergence* on the commensurate side of the transition. The transverse correlation length in the incommensurate phase must be simply proportional to  $l$  and hence may be written as<sup>(2)</sup>

$$\xi_{\perp} \approx b_{\perp}/t^{\nu_{\perp}} \quad \text{with} \quad \nu_{\perp} = \bar{\beta} = \frac{1}{2} \tag{12.10}$$

and, thence, via the diffusive character of the walk as seen previously,

$$\xi_{\parallel} \approx c(l/b)^2 \approx c_{\parallel}/t^{\nu_{\parallel}} \quad \text{with} \quad \nu_{\parallel} = 2\nu_{\perp} = 1 \tag{12.11}$$

These results are in agreement with the fermion type of analysis.<sup>(62)</sup> Evidently the anisotropic hyperscaling relation

$$2 - \alpha = \nu_{\parallel} + \nu_{\perp} \tag{12.12}$$

is satisfied. One can generalize these arguments by including an ordering field,  $h$ , which favors one type of commensurate domain: this is found to scale with an exponent  $\Delta = 1\frac{1}{2}$ .<sup>(2)</sup>

It is interesting that the result for the specific heat, including its characteristic asymmetry with no divergence below  $T_c$ , can be verified by exact calculations for what is, on the face of it, a completely different type of model. Consider the *dimer problem* in which “hard dimers” occupy the bonds of a lattice (and the two associated terminal sites). If a planar lattice is filled with dimers the partition function can be calculated exactly by Pfaffian methods.<sup>(64–66)</sup> In particular, Kasteleyn,<sup>(67)</sup> has considered a brick (or, equivalently, honeycomb) lattice, as illustrated in Fig. 21, in which

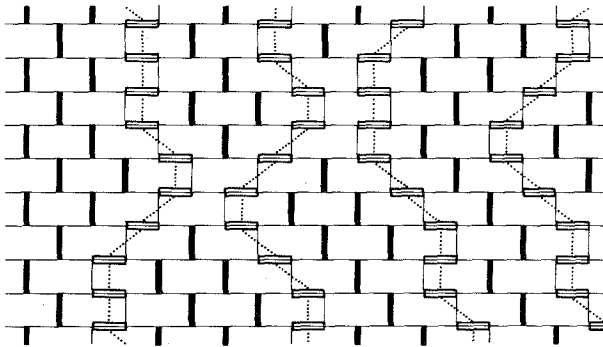


Fig. 21. Dimer problem on a brick lattice in which vertical dimers (bold) have a different chemical potential than horizontal dimers. The dotted lines indicate that a configuration of horizontal dimers can always be regarded as composed of nonintersecting strings or walks running, on average, vertically.

dimers on vertical or  $y$  bonds have different statistical weights or a chemical potential excess, say,  $\Delta\mu$ . This dimer model has a transition when  $\Delta\mu/k_B T_c = \ln 2$ . The low-temperature phase is “frozen,” all dimers pointing “up,” i.e., parallel to the  $y$  axis, and the specific heat vanishes; above  $T_c$ , however, horizontal dimers are present and the specific heat diverges as  $t^{-\frac{1}{2}}$ .<sup>(67)</sup>

Why do these results confirm the heuristic analysis leading to (12.8) and (12.9)? The answer is contained in Fig. 21 which serves to demonstrate that horizontal dimers can appear *only* in nearest-neighbor strings that run, on average, vertically through the lattice. An isolated string can be regarded as a domain wall in a  $p \times 1$  commensurate phase with  $p = 1$ ; above  $T_c$  the state of many walls clearly corresponds to the associated incommensurate phase. (Note that the heuristics gives  $\alpha = \frac{1}{2}$  and  $\bar{\beta} = \frac{1}{2}$  independently of  $p$ .) Once again, then, the simple picture of domain walls in two dimensions which interact through a  $1/l^2$  potential reproduces the exact asymptotic behavior!

### 13. DISLOCATIONS AND THEIR EFFECTS

The account just presented of the commensurate–incommensurate transition neglected completely the possibility that the array of domain walls might exhibit any type of topological defect formed by some of the walls merging. In a  $p \times 1$  phase the elementary defects consist of *dislocations* (or *vortices*) at which  $p$  walls come together and terminate. Allowing for such dislocations, say, with an activity  $v$ , alters the picture of both the

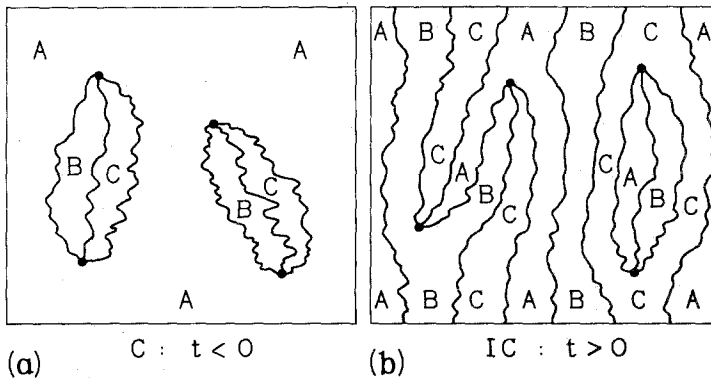


Fig. 22. Representation of (a) fluctuations arising in a  $3 \times 1$  commensurate phase close to the C–IC transition when dislocations are allowed and (b) configurations of domain walls in the corresponding incommensurate phase when dislocations are present.

commensurate and the incommensurate phases. In the former case, as illustrated in Fig. 22a for  $p = 3$ , heterodomain fluctuations arise which prefigure the nature of the new, incommensurate phase.<sup>(2)</sup><sup>24</sup> On the other hand, as illustrated in Fig. 22b, dislocations can appear in various ways in the incommensurate phase<sup>(42,63)</sup> and should be considered in giving a full account of its properties. Indeed, one must ask if the presence of dislocations for  $v > 0$  might not change the nature of the singularities at the C-IC transition,<sup>(2)</sup> or even destroy the incommensurate phase altogether!<sup>(42,63)</sup>

Physically, dislocations must always be allowed for even if, in practice,  $v$  turns out to be small. Ideally, however, one may consider  $v = 0$ ; indeed, the brick lattice dimer model corresponds to this situation since one can easily check from Fig. 21 that *no* dislocations can occur there. For  $v = 0$  we may accept the previous theory of C-IC transition (as checked by the exact model results<sup>(40,67)</sup> and then ask<sup>(2)</sup> “Does the dislocation activity,  $v$ , represent a *relevant* or *irrelevant* perturbation of the transition in the renormalization group sense?”<sup>(11,68-71)</sup> More concretely, with  $t$  defined as in (12.2) the scaling form

$$f_s(t, v) \approx |t|^{3/2} \Upsilon_{\pm}(v/|t|^{\phi_p}) \quad (13.1)$$

should hold for small  $v$ . Here  $\Upsilon_{\pm}(z)$  represents the scaling function for  $t \rightarrow 0 \pm$  while  $\phi_p$  is the appropriate *crossover scaling exponent*.<sup>(11,68,70)</sup> If  $\phi_p$  is negative  $v$  is irrelevant and only higher-order corrections to the transition behavior should arise; positive  $\phi_p$ , on the other hand, implies that  $v$  is relevant which implies that the transition is destroyed or, at least, changed in character.

Now,<sup>(2)</sup> from (13.1) we have

$$f_0'' \equiv \left( \frac{\partial^2 f_s}{\partial v^2} \right)_{v=0} \approx \Upsilon_{-}''(0) |t|^{3/2-2\phi_p} \quad (13.2)$$

for  $t < 0$ . On the other hand,<sup>(2)</sup> if we expand the full partition function for the commensurate phase to quadratic order in  $v$  we see that  $f_0''$  is proportional to the total partition function,  $Z_2^p$  for a single “bubble” of  $p$  strands terminated by two dislocations, as illustrated in Fig. 22a. But the partition function,  $\Theta_p(x, y)$ , for a bubble with one dislocation at  $(0, 0)$  and one at  $(x, y)$  can be described by the reunions of  $p$  walkers where, as before, the step weight  $\sigma$  represents the reduced surface tension for a wall parallel to the  $y$  axis, which, by (12.5), vanishes like  $|t|$  when the transition is

<sup>24</sup> It is instructive to compare Fig. 22a with Fig. 13 and to note that, as seems physically reasonable, we consider only one type of wall near the incommensurate phase transition, i.e., we suppose the transition occurs from a fully *wet* region of the commensurate phase.

approached. Thus, for  $t < 0$ , we have

$$\begin{aligned} Z_2^p(T) &= \int dx \int dy \Theta_p(x, y) \approx \sum_n e^{-p\sigma n} R_n^{(p)} \\ &\approx C_p \sum_n e^{+p\sigma_1 t n} / n^\psi \quad \text{with} \quad \psi = \frac{1}{2}(p^2 - 1) \end{aligned} \quad (13.3)$$

where we have appealed to the walk result (4.16). The leading singular behavior follows as in (6.11) and is proportional to  $|t|^{\psi-1}$  but with a factor  $\ln|t|$  when  $\psi$  is an integer. Comparing with (13.2) finally yields the crossover exponent<sup>(2)</sup>

$$\phi_p = \frac{1}{4}(6 - p^2) \quad (13.4)$$

Now for  $p = 1$  or  $2$  we see that  $\phi_p$  is positive so that  $v$  is *relevant*. In fact, dislocations then destroy the incommensurate phase altogether as one may anticipate from the explicit results for Ising models which describe the cases  $p = 1$  or  $2$ : only a commensurate ordered phase and disordered fluid phases are seen.<sup>(2)</sup> Conversely, for  $p \geq 3$  the dislocations are irrelevant, and the incommensurate phase should remain stable for  $v > 0$ . These conclusions agree with the analysis of Coppersmith *et al.*<sup>(42)</sup> and Villain and Bak<sup>(63)</sup> (who, however, primarily address the question of the stability of the incommensurate phase not too close to the transition itself).

Even though the dislocations are technically irrelevant for  $p \geq 3$  one sees from (13.1) that they lead to correction-to-scaling factors of the form

$$\left[ a_0^\pm + a_1^\pm |t|^{\theta_p} + a_2^\pm |t|^{2\theta_p} + \dots \right] \quad \text{with} \quad \theta_p = \frac{1}{4}(p^2 - 6) \quad (13.5)$$

In the commensurate phase ( $t < 0$ ), however, only even powers of  $|t|^{\theta_p}$  appear, since dislocations must occur in bound pairs; furthermore, when  $2\theta_p$  is integral a factor  $\ln|t|$  enters. Since  $2\theta_p = 1\frac{1}{2}$  and  $5$  for  $p = 3$  and  $4$ , respectively, the corrections are of relatively high order. Nevertheless, they should be visible for  $p = 3$  since, as seen in the previous section, the leading singularities vanish identically on the commensurate side of the transition so that the "corrections" actually play the dominant role! Thus one finds that the specific heat should exhibit<sup>(2)</sup> a  $|t|\ln|t|$  behavior below  $T_c$ , which, as sketched in Fig. 23, represents a cusp with vertical slope in contrast to the  $|t|^{-1/2}$  behavior above  $T_c$ . Likewise, one can show<sup>(2)</sup> that the ordering susceptibility, which diverges like  $|t|^{-3/2}$  in the incommensurate phase, should diverge as  $\ln|t|^{-1}$  below the transition.

In principal, one might hope to observe the dislocation-dislocation correlation function,  $C_2^p(x, y)$ . In the commensurate phase near the transition this follows from the reunion distribution (4.12). If one scales the  $x$  and  $y$  coordinates in accord with (12.10) and (12.11) by writing

$$X = x/\xi_\perp \approx x|t|^{1/2}/b_1, \quad Y = y/\xi_\parallel \approx y|t|/c_1 \quad (13.6)$$

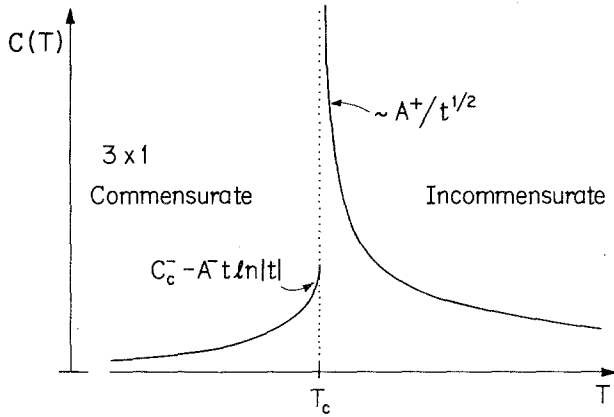


Fig. 23. Sketch showing the variation of the specific heat through a  $3 \times 1$  commensurate-incommensurate transition when dislocations can be generated. In the absence of dislocations the specific heat below  $T_c$  should be smooth and analytic.

one finds a scaling form

$$C_2^p(x, y) \approx c_p |t|^{\frac{1}{2}p^2} \Gamma_{\pm}(X, Y) \tag{13.7}$$

where the walk distribution yields<sup>(2)</sup>

$$\Gamma_{-}(X, Y) = e^{-pR} / R^{\frac{1}{2}p^2} \quad \text{with} \quad R^2 = X^2 + Y^2 \tag{13.8}$$

for  $t < 0$  and  $X^2 = O(Y)$ . (The coefficient  $c_p$  is a nonuniversal amplitude.) Schultz, Halperin, and Henley<sup>(72)</sup> have used fermion methods for  $t > 0$  to obtain

$$\Gamma_{+}(X, Y) \sim 1 / R^{\frac{1}{2}p^2} \quad \text{as} \quad R \rightarrow \infty \tag{13.9}$$

but note that this applies only for  $r \gg \xi_{||} \sim l^2/b$ .<sup>(2)</sup> More generally, the behavior of the dislocation-dislocation correlation function in the incommensurate phase requires an analysis of domain wall configurations such as shown in Fig. 22b. This is beyond the present scope of our random walk formulation but one may hope that the approach can be extended to yield similarly transparent results for the reunions of walkers moving within a sea of other walkers!

#### 14. MORE THAN TWO DIMENSIONS? LIPID MEMBRANES

The applications of random walks and their interactions which we have studied so far have been restricted to physical systems of two or fewer dimensions. To close our study let us ask if one can obtain interesting

results by similar means for systems of higher dimensions? Two obvious lines of development present themselves. A domain wall separating  $d$ -dimensional bulk phases is a curve for  $d = 2$ , and hence representable as a trajectory of a walker, but a *surface* for  $d = 3$ . One would, thus, like to study self-avoiding surfaces and the interactions between such surfaces and a wall or between two or more surfaces which may not intersect one another. This is a difficult problem even if it is simplified, in analogy with our treatment for  $d = 2$ , by regarding one dimension as time-like and examining the motion of a self-avoiding chain which lies in a plane. In fact, some heuristic arguments applicable to the commensurate-incommensurate transition have been developed.<sup>(43,44)</sup> In addition, some foundations for a rigorous theory have been laid out recently.<sup>(73)</sup> However, no fully convincing explicit results seem available.

On the other hand, one may enquire after the properties of one-dimensional interacting strings or chains which are embedded in three or more dimensions. If, as illustrated in Fig. 24a, a three-dimensional system is uniaxial with the strings lying, on average, parallel to one (time-like) axis, they may be regarded as the trajectories of vicious walkers moving in a plane. A model for which this picture is relevant has recently been proposed by Izuyama and Akutsu,<sup>(74)</sup> who studied it using approximate methods. Following earlier work by Nagle,<sup>(75)</sup> who adapted Kasteleyn's dimers-on-a-brick-lattice<sup>(67)</sup> to describe interacting lipid and polymer mole-

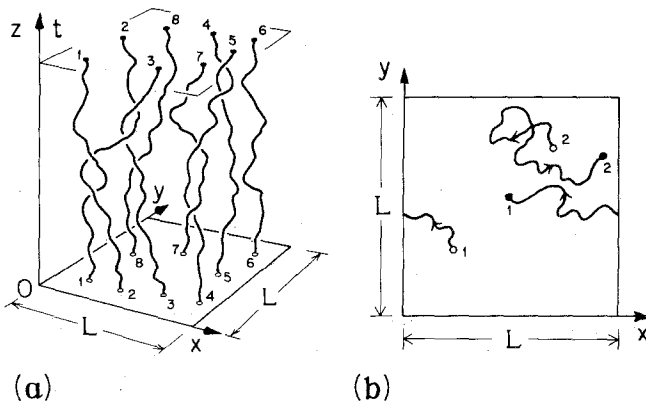


Fig. 24. (a) A configuration of nonintersecting strings which lie predominantly parallel to the  $z$  axis but wander in the  $(x, y)$  directions. The strings may be interpreted as dislocation lines in the Izuyama-Akutsu model of a lipid membrane. (b) Paths of two vicious walkers on a two-dimensional  $L \times L$  torus. Although the walkers cannot *meet*, their trails may cross in the  $(x, y)$  plane; however, their trajectories in  $(x, y, t \equiv z)$  space will not intersect.

cules in two dimensions, Izuyama and Akutsu introduced a similar dimer model for bulk, three-dimensional lipid membranes which undergo a thermal melting transition. In their model, square lattice layers are stacked vertically and connected in brick-like fashion (generalizing Fig. 21).<sup>(74)</sup> This lattice is filled with dimers but vertical dimers again enjoy an excess chemical potential, say,  $\Delta\mu (> 0)$ . As in two dimensions, it is easy to see that the low-temperature phase is completely frozen, with all dimers in a vertical orientation, but that a melting transition occurs when  $\Delta\mu/k_B T = \ln 4$ . Above  $T_c$  horizontal dimers appear but, as in Fig. 21, their only possible configurations are such that they can be regarded as defining strings or “dislocation lines;” as suggested in Fig. 24a, these strings must run vertically through the lattice but may wander sideways in the layers provided they do not intersect one another. The nature of this membrane melting transition has not, as yet, been convincingly determined. Inspired by the success of simple heuristic ideas in two dimensions, we may, however, attack the problem as follows.<sup>(76)</sup>

Suppose the cross-section of the system transverse to the principal axis has dimensions  $L \times L$ , as indicated in Fig. 24a, and that there are  $N$  strings in the system which repel one another via a pair potential  $W(r)$  depending on their mutual separations,  $r$ . If  $l = L/N^{1/2}$  is the mean interstring spacing and the reduced tension of a single string is  $\sigma \approx -\sigma_1 t$ , with  $t \propto (T - T_c)$ , the free energy density, as in Section 12, may be expressed phenomenologically by

$$f(T; l) \approx \frac{1}{L^2} \left[ N\sigma + jN \frac{W(l)}{k_B T} \right] \approx -\frac{\sigma_1 t}{l^2} + \frac{jW(l)}{l^2 k_B T} \quad (14.1)$$

where  $j$  is a geometric factor accounting for the mean coordination number and further neighbor interactions.

So far so good; but how are we to determine the interaction potential  $W(r)$ ? This task may be approached in two steps<sup>(76)</sup>: first, in analogy with our arguments for walkers on a line, consider the case  $N = 2$ , illustrated in Fig. 24b. Two vicious walkers, who must not meet, move in two-dimensions within a square of side  $L$ . To simplify the problem let us take periodic boundary conditions, so that the “square” is really a torus, as suggested in the figure. To determine  $W(r)$  we note that the mean separation of the walkers is  $l = L/\sqrt{2}$  and ask for the incremental free energy of the system over the value  $2\sigma$  for two widely separated strings ( $L \rightarrow \infty$ ). The problem of two vicious walkers on a torus can be simplified by going to center-of-mass coordinates (as used to discuss two dissimilar walkers on a line): this yields one free walker on a torus and one “internal” walker who must not visit the origin of the torus. This latter problem can be solved exactly along the lines

used in proving (2.9). With due care the requisite asymptotic analysis can be performed for large  $L$  and yields<sup>(76)</sup>

$$W(L/\sqrt{2}) \approx \pi b^2/L^2 \ln(L/b) \quad \text{for} \quad N = 2 \quad (14.2)$$

Now this result, although exact, applies only for  $N = 2$  walkers and  $L \rightarrow \infty$ , i.e., to a situation of asymptotically zero density; however, we really require  $W(l)$  for small but nonzero overall density,  $\rho = N/L^2 = 1/l^2$ . In order to leap this gap we may introduce what is essentially a strong finite-size scaling ansatz,<sup>(57,77)</sup> namely, we suppose that (14.2) remains true for large but finite  $l$ , at least up to some proportionality factor, if  $L$  is replaced by  $\sqrt{2}l$ . Thereby we conclude that the potential varies for large  $l/b$  as

$$W(l) \approx \pi b_0^2/l^2 \ln(l/b_0) \quad (14.3)$$

where  $b_0 \simeq b/\sqrt{2}$ .

If one accepts this reasoning, one can proceed to minimize  $f(T; l)$  with respect to  $l$  and thence determine the critical behavior of the free energy. One finds that the specific heat above the transition varies as<sup>(76)</sup>

$$C(T) \propto \frac{\partial}{\partial T} \left( \frac{b_0^2}{l^2} \right) \approx A_0 \ln t^{-1} + \dots \quad (14.4)$$

In other words, the transition is critical with  $\alpha = 0$  and a logarithmically divergent specific heat!<sup>(76)</sup>

More generally, if one carries through the analogous argument for a  $d$ -dimensional system, regarding  $d$  as a continuous variable, one finds  $\alpha = \frac{1}{2}(3 - d)$  for  $1 < d < 3$ . Note that this reproduces correctly the original result  $\alpha = \frac{1}{2}$  for  $d = 2$  [see (12.9)]. On the other hand, for all  $d > 3$  one obtains  $\alpha = 0$  but with  $C(T)$  bounded as  $T \rightarrow T_c +$ , i.e., classical, second-order critical behavior. Thus  $d = 3$  represents the upper *borderline dimension* for the lipid membrane melting transition. As such one is not surprised to see logarithmic factors appearing.<sup>(69,70)</sup> Nevertheless, some caution is in order since experience with systematic renormalization group analyses<sup>(69,70)</sup> indicates that nontrivial powers of logarithms may appear. Consequently, although (14.4) is most appealing and suggestive it cannot be regarded as definitive.

Clearly, then, the problem of interacting walkers moving in more than one dimension demands further study: the walkers' paths may tangle seriously but one may hope that diligence will be rewarded by the unraveling of some further problems!

## ACKNOWLEDGMENTS

Much of the research work reviewed above was performed in close association with David A. Huse whose collaboration was much appreciated. I am grateful to Daniel S. Fisher for rekindling my interests in random walks and alerting me to new developments. Some of my first lessons in random walk theory came from Cyril Domb, whose tutelage and early encouragement I would like to acknowledge particularly on this occasion. The stimulation provided by many other colleagues through personal contacts and communications and through the media of preprint and reprint has been important to me: I regret I cannot acknowledge all by name. Anthony M. Szpilka participated in some of the researches reported and kindly commented in detail on the manuscript. I am grateful to the Institut des Hautes Études Scientifiques for hospitality during a visit when the lecture on which this article is based was prepared. Last but not least, I am indebted to the National Science Foundation for ongoing support, provided in part through the Materials Science Center at Cornell University.

## REFERENCES

1. W. Feller, *An Introduction to Probability Theory and its Applications*, Vol. 1 (John Wiley & Sons, New York, 1950).
2. D. A. Huse and M. E. Fisher, *Phys. Rev. B* **29**:239 (1984).
3. D. A. Huse, A. M. Szpilka, and M. E. Fisher, *Physica* **121A**:363 (1983).
4. P.-G. de Gennes, *J. Chem. Phys.* **48**:2257 (1968).
5. F. J. Dyson, *Commun. Math. Phys.* **21**:269 (1971).
6. J. Fröhlich and T. Spencer, *Commun. Math. Phys.* **84**:87 (1982).
7. M. E. Fisher, *Physics* **3**:255 (1967).
8. M. E. Fisher and B. U. Felderhof, *Ann. Phys. (N. Y.)* **58**:176, 217, 268, 281 (1970).
9. H. N. V. Temperley, *Phys. Rev.* **103**:1 (1956).
10. M. E. Fisher, *Rept. Prog. Phys.* **30**:615 (1967).
11. M. E. Fisher, *Proc. Nobel Symp.* **24**, *Collective Properties of Physical Systems*, B. Lundqvist and S. Lundqvist, eds. (Academic Press, New York, 1974), p. 16.
12. J. W. Cahn, *J. Chem. Phys.* **66**:3667 (1977).
13. C. Ebner and W. F. Saam, *Phys. Rev. Lett.* **38**:1486 (1977).
14. D. B. Abraham, *Phys. Rev. Lett.* **44**:1165 (1980).
15. J. D. Weeks, in *Ordering in Strongly Fluctuating Condensed Matter Systems*, T. Riste, ed. (Plenum, New York, 1980), p. 293.
16. S. T. Chui and J. D. Weeks, *Phys. Rev. B* **23**:2438 (1981).
17. T. W. Burkhardt, *J. Phys. A* **14**:L63 (1981).
18. J. M. J. van Leeuwen and H. J. Hilhorst, *Physica* **107A**:319 (1981).
19. H. N. V. Temperley, *Proc. Cambridge Philos. Soc.* **48**:683 (1952).
20. D. A. Huse and M. E. Fisher, *Phys. Rev. Lett.* **49**:793 (1982).
21. M. R. Moldover and J. W. Cahn, *Science* **207**:1073 (1980).
22. O'D. Kwon, D. Beaglehole, W. W. Webb, B. Widom, J. W. Schmidt, J. W. Cahn, M. R. Moldover and B. Stephenson, *Phys. Rev. Lett.* **48**:185 (1982).

23. D. W. Pohl and W. I. Goldberg, *Phys. Rev. Lett.* **48**:1111 (1982).
24. J. W. Schmidt and M. R. Moldover, *J. Chem. Phys.* **79**:379 (1983).
25. J. S. Rowlinson and B. Widom, *Molecular Theory of Capillarity* (Clarendon Press, Oxford, 1982).
26. D. Poland and H. A. Scheraga, *Theory of Helix-Coil Transitions in Biopolymers* (Academic Press, New York, 1970).
27. C. L. Stevens and G. Felsenfeld, *Biopolymers* **2**:293 (1964).
28. M. E. Fisher, *J. Chem. Phys.* **45**:1469 (1966).
29. J. G. Dash and J. Ruvalds, eds., *Phase Transitions in Surface Films* (Plenum Press, New York, 1980).
30. R. Imbuhl, R. J. Behm, K. Christmann, G. Ertl, and T. Matsushima, *Surf. Sci.* **117**:257 (1982).
31. M. Bretz, *Phys. Rev. Lett.* **38**:501 (1977).
32. D. E. Moncton, P. W. Stephens, R. J. Birgeneau, P. M. Horn, and G. S. Brown, *Phys. Rev. Lett.* **46**:1533 (1981); **49**:1679 (1982).
33. S. Alexander, *Phys. Lett.* **54A**:353 (1975).
34. E. Domany, M. Schick, J. S. Walker, and R. B. Griffiths, *Phys. Rev. B* **18**:2209 (1978).
35. R. J. Baxter, *J. Stat. Phys.* **26**:427 (1981).
36. R. J. Baxter and P. A. Pearce, *J. Phys. A* **15**:897 (1982); **16**:2239 (1983).
37. M. Stone, *Phys. Rev. D* **23**:1862 (1981).
38. S. Ostlund, *Phys. Rev. B* **24**:398 (1981); **23**:2235 (1981).
39. D. A. Huse, *Phys. Rev. B* **24**:5180 (1981).
40. V. L. Pokrovsky and A. L. Talapov, *Zh. Eksp. Teor. Fiz.* **78**:269 (1980) [*Sov. Phys. JETP* **51**:134 (1980)].
41. J. Villain and M. Gordon, *J. Phys. C* **13**:3117 (1980); F. D. M. Haldane and J. Villain, *J. Phys. (Paris)* **42**:1673 (1981).
42. S. N. Coppersmith, D. S. Fisher, B. I. Halperin, P. A. Lee, and W. F. Brinkman, *Phys. Rev. Lett.* **46**:549 (1981); *Phys. Rev. B* **25**:349 (1982).
43. M. E. Fisher and D. S. Fisher, *Phys. Rev.* **25**:3192 (1982).
44. T. Nattermann, *J. Phys. (Paris)* **43**:631 (1982); *J. Phys. C* **16**:4125 (1983).
45. R. Pandit and M. Wortis, *Phys. Rev. B* **25**:3226 (1982).
46. H. Nakanishi and M. E. Fisher, *Phys. Rev. Lett.* **49**:1565 (1982).
47. D. B. Abraham and E. R. Smith, *Phys. Rev. B* **26**:1480 (1982).
48. W. J. Camp and M. E. Fisher, *Phys. Rev. Lett.* **26**:73 (1971); *Phys. Rev. B* **5**:946 (1972).
49. T. T. Wu, *Phys. Rev.* **149**:380 (1966).
50. L. P. Kadanoff, *Nuovo Cimento* **44B**:276 (1966).
51. R. Hartwig and M. E. Fisher, *Adv. Chem. Phys.* **15**:333 (1969).
52. B. M. McCoy and T. T. Wu, *The Two-dimensional Ising Model* (Harvard University Press, Cambridge, Massachusetts, 1973).
53. H. B. Tarko and M. E. Fisher, *Phys. Rev. B* **11**:1217 (1975).
54. W. J. Camp, *Phys. Rev. B* **6**:960 (1972).
55. M. E. Fisher and W. J. Camp, *Phys. Rev. Lett.* **26**:565 (1971).
56. B. M. McCoy and T. T. Wu, *Phys. Rev. D* **18**:1259, 1243, 1253 (1978).
57. D. B. Abraham, *Phys. Rev. Lett.* **50**:291 (1983).
58. M. E. Fisher and A. E. Ferdinand, *Phys. Rev. Lett.* **19**:169 (1967).
59. D. B. Abraham, G. Gallavotti, and A. Martin-Löf, *Physica* **65**:73 (1973).
60. P. Bak, *Rept. Prog. Phys.* **45**:587 (1982).
61. P. Bak and V. J. Emery, *Phys. Rev. Lett.* **36**:978 (1976).
62. H. J. Schulz, *Phys. Rev. B* **22**:5274 (1980); *Phys. Rev. Lett.* **46**:1685 (1981).
63. J. Villain and P. Bak, *J. Phys. (Paris)* **42**:657 (1981).

64. P. W. Kasteleyn, *Physica* **27**:1209 (1961).
65. H. N. V. Temperley and M. E. Fisher, *Philos. Mag.* **6**:1061 (1961).
66. M. E. Fisher, *Phys. Rev.* **124**:1664 (1961).
67. P. W. Kasteleyn, *J. Math. Phys.* **4**:287 (1964).
68. F. J. Wegner, *Phys. Rev. B* **5**:4529 (1972).
69. K. G. Wilson and J. Kogut, *Phys. Rept.* **12C**:75 (1974).
70. M. E. Fisher, *Rev. Mod. Phys.* **46**:597 (1974).
71. K. G. Wilson, *Rev. Mod. Phys.* **47**:773 (1975); **55**:583 (1983).
72. H. J. Schulz, B. I. Halperin, and C. L. Henley, *Phys. Rev. B* **26**:3797 (1982).
73. B. Durhuus, J. Fröhlich, and T. Jonsson (preprint, 1983).
74. T. Izuyama and Y. Akutsu, *J. Phys. Soc. Japan* **51**:50, 730 (1982).
75. J. F. Nagle, *Ann. Rev. Phys. Chem.* **31**:157 (1980); *Proc. R. Soc. London Ser. A* **337**:569 (1974).
76. S. M. Bhattacharjee, J. F. Nagle, D. A. Huse, and M. E. Fisher, *J. Stat. Phys.* **32**:361 (1983).
77. M. E. Fisher, in *Critical Phenomena*, Proceedings of the 1970 Enrico Fermi International School of Physics, Course No. 51, Varenna, M. S. Green, ed. (Academic Press, New York, 1971), p. 1.